ELSEVIER

Chemistry & Biology 8 (2001) 681–700

Chemistry & Biology

www.elsevier.com/locate/chembiol

Research Paper

Insights about the biosynthesis of the avermectin deoxysugar L-oleandrose through heterologous expression of *Streptomyces avermitilis* deoxysugar genes in *Streptomyces lividans*

Sven-Eric Wohlert [a], Natalia Lomovskaya [a], Kerry Kulowski [a], Leonid Fonstein [a], James L. Occi [b], Keith M. Gewain [b], Douglas J. MacNeil [b], C. Richard Hutchinson [a,c,*]

[a] *School of Pharmacy, University of Wisconsin, 425 N. Charter St., Madison, WI 53706, USA*
[b] *Department of Metabolic Disorders, Merck Research Labs., Rahway, NJ 07065, USA*
[c] *Department of Bacteriology, University of Wisconsin, 425 N. Charter St., Madison, WI 53706, USA*

Received 24 January 2001; revisions requested 9 March 2001; revisions received 20 April 2001; accepted 27 April 2001
First published online 7 June 2001

Abstract

Background: The avermectins, produced by *Streptomyces avermitilis*, are potent anthelminthic agents with a polyketide-derived macrolide skeleton linked to a disaccharide composed of two α-linked L-oleandrose units. Eight contiguous genes, *avrBC-DEFGHI* (also called *aveBI–BVIII*), are located within the avermectin-producing gene cluster and have previously been mapped to the biosynthesis and attachment of thymidinediphospho-oleandrose to the avermectin aglycone. This gene cassette provides a convenient way to study the biosynthesis of 2,6-dideoxysugars, namely that of L-oleandrose, and to explore ways to alter the biosynthesis and structures of the avermectins by combinatorial biosynthesis.

Results: A *Streptomyces lividans* strain harboring a single plasmid with the *avrBCDEFGHI* genes in which *avrBEDC* and *avrIHGF* were expressed under control of the *actI* and *actIII* promoters, respectively, correctly glycosylated exogenous avermectin A1a aglycone with identical oleandrose units to yield avermectin A1a. Modified versions of this minimal gene set produced novel mono- and disaccharide avermectins. The results provide further insight into the biosynthesis of L-oleandrose.

Conclusions: The plasmid-based reconstruction of the *avr* deoxysugar genes for expression in a heterologous system combined with biotransformation has led to new information about the mechanism of 2,6-deoxysugar biosynthesis. The structures of the di-demethyldeoxysugar avermectins accumulated indicate that in the oleandrose pathway the stereochemistry at C-3 is ultimately determined by the 3-*O*-methyltransferase and not by the 3-ketoreductase or a possible 3,5-epimerase. The AvrF protein is therefore a 5-epimerase and not a 3,5-epimerase. The ability of the AvrB (mono-)glycosyltransferase to accommodate different deoxysugar intermediates is evident from the structures of the novel avermectins produced.

Keywords: *avr* Gene; Biotransformation; Deoxysugar biosynthesis; Glycosyltransferase; Methyltransferase; Epimerase; Avermectin; Mycarose; Oleandrose; Combinatorial biosynthesis

1. Introduction

Microorganisms, particularly *Actinomycetes*, produce complex natural products that are often decorated with highly modified deoxyhexoses. Some of the most important antibiotic and antitumor agents, such as the erythromycins, vancomycin, and doxorubicin, lack substantial activity without the attached deoxysugars. In contrast, the series of anthelminthic, 16-membered macrolides produced by *Streptomyces hygroscopicus* (milbemycins) and *Streptomyces thermoachaensis* (nemadectins) (Fig. 1) are potent anthelminithic agents whose structures are closely related to the avermectins (*Streptomyces avermitilis*), but do not have sugars attached. Removing the oleandrose disaccharide attached at the C-13 position of avermectin macrolide causes a considerable decrease in activity even though it is not strictly required for activity [1–4]. Recognition of the

* Correspondence: C. Richard Hutchinson. Present address: Kosan Biosciences, Inc., 3832 Bay Center Place, Hayward, CA 94545, USA; E-mail: hutchinson@kosan.com

1074-5521/01/$ – see front matter
PII: S1074-5521(01)00043-6

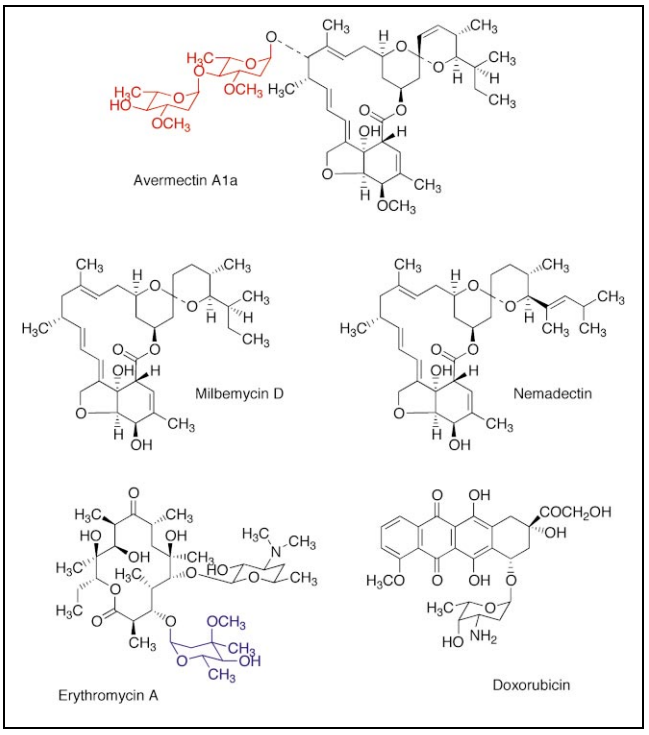

Fig. 1. Structures of different antibiotic and antitumor agents.

importance of deoxysugars for the bioactivity of antibiotics and antitumor agents has caused a growing interest in their biosynthesis over the last years [5–8].

Genetic analysis of *S. avermitilis* has revealed eight genes, *avrBCDEFGHI*, that by mutations [1,9–11] and DNA sequence analysis [12,13] have been assigned to the biosynthesis of thymidinediphospho (TDP)-oleandrose and its transfer to avermectin aglycones. Ikeda et al. [13] have recently named these genes as *aveBI–BVIII*, respectively. This cluster of contiguous genes provides a convenient system for studying the biosynthesis of neutral 2,6-dideoxysugars by biotransformation studies in a heterologous host. The cluster can be restructured on self-replicating plasmids and expressed with artificial promoters to investigate the role of the individual genes in oleandrose biosynthesis and glycosylation of the avermectin aglycones. One or more of the genes can be removed from the plasmid or be replaced with homologs from other bacteria to survey the possibility of creating analogs of the avermectins or other glycosidic metabolites by combining steps from different deoxysugar biosyntheses. Although it is not known whether avermectins with modified glycosides will have improved properties, the ability to make manifold changes in the deoxysugar portion of these and other macrolide antibiotics would certainly further the quest for new drugs.

To accomplish this goal, the first step was to outline the role for each of the *avr* genes in L-oleandrose biosynthesis, following the suggestions made by the Merck group [1,12] and researchers at the Kitasato Institute [2,13,14]. The biosynthetic pathway of L-oleandrose has a close analogy to that of the structurally related L-mycarose, as found in macrolides like the erythromycins [15–18] and the tylosins [19,20] (Table 1), while L-oleandrose is also found in oleandomycin [21]. As illustrated in Fig. 2, the first two steps in the oleandrose and mycarose pathways involve conversion of glucose-1-phosphate to its TDP form by a thymidylyl transferase (*avrD*/*aveBII*) and then to TDP-4-keto-6-deoxyglucose by a dehydratase (*avrC*/*aveBIII*). These two steps are common to the formation of all 6-deoxyhexoses in bacteria [5–8], even though the corresponding genes do not always lie in the same cluster as the rest of the deoxysugar biosynthesis genes for a given secondary metabolite, as in case of erythromycin. For oleandrose and mycarose, C-2 deoxygenation takes place next – as shown by Floss et al. [22] and Liu et al. [20] – involving *avrG*/*aveBVI* (encoding a C-2,3-dehydratase) and *avrI*/*aveBVIII* (encoding a C-3-ketoreductase) or the homologous *eryBVI* and *eryBII* genes.

The proposed biosynthetic pathway for TDP-L-oleandrose then modifies the TDP-2,6-dideoxy-4-ketoglucose by the AvrF/AveBV C-(3)5-epimerase, AvrH/AveBVII C-3-*O*-methyltransferase, and AvrE/AveBIV C-4-ketoreductase. For TDP-L-mycarose, the *eryBVII* and *eryBIV* genes control the epimerization and ketoreduction steps [15–18], whereas *eryBIII* is believed to encode the C-3-*C*-methyltransferase [18]. The order in which each of these three reactions occurs is unknown though, as mentioned above, the 2-deoxygenation step follows 4,6-dehydration [20,22].

Table 1
Functional assignments for genes associated with the biosynthesis of oleandrose in *S. avermitilis* and mycarose in *S. erythraea* and *S. fradiae*

Gene[a]	Function[b]	Amino acid sequence comparisons (% similarity/% identity)
avrB/*aveBI*	glycosyltransferase	EryBV (45/21), TylCV (57/39)
avrC/*aveBII*	TDP-glucose 4,6-dehydratase	EryGdh (83/69)
avrD/*aveBIII*	glucose-1-phosphate-thymidylyltransferase	none in erythromycin genes
avrE/*aveBIV*	TDP-4-ketohexulose reductase	EryBIV (66/50), TylCIV(51/30), TylD (50/30)
avrF/*aveBV*	TDP-4-keto-6-deoxyglucose 3-epimerase	EryBVII (71/55), TylJ (63/46), TylCVII (58/43)
avrG/*aveBVI*	TDP-4-keto-6-deoxyglucose 2,3-dehydratase	EryBVI (66/47)
avrH/*aveBVII*	TDP-6-deoxy-L-hexose 3-*O*-methyltransferase	EryBIII (51/19), TylE (51/25), TylF (46/20)
avrI/*aveBVIII*	TDP-4-keto-6-deoxy-L-hexose 3-ketoreductase	EryBII (73/61), TylCII (73/60)

[a]The genes are listed in the order they occur in the avermectin gene cluster.
[b]As proposed in the references cited in the text.

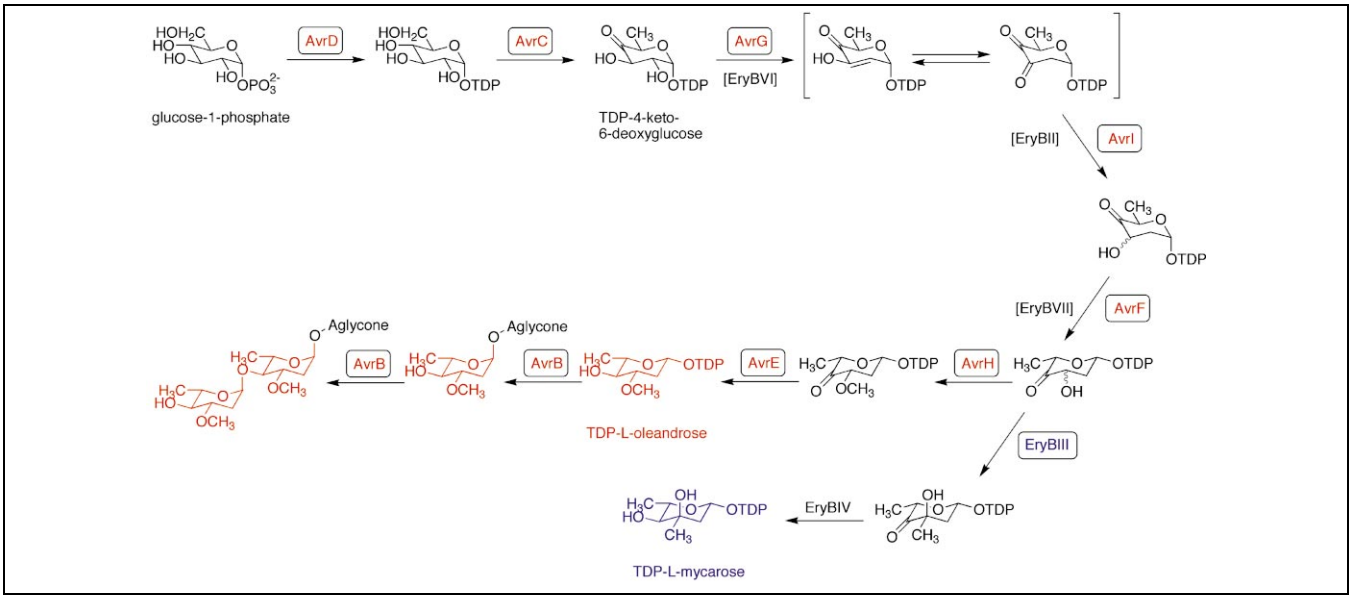

Fig. 2. Proposed pathway for the biosynthesis of L-oleandrose and L-mycarose.

We therefore favor the order of reactions as shown in Fig. 2. The same order has also been proposed by Salas and coworkers in their study of the oleandrose biosynthesis and glycosyltransferase genes in the oleandomycin producer [23]. Raynal et al. [18] have proposed a different sequence of reactions for mycarose. They propose that TDP-4-keto-6-deoxyglucose undergoes epimerization by EryBVII, followed by 2,3-dehydration (EryBVI) and reduction (EryBII), C-methyl transfer (EryBIII) and finally reduction of the 4-keto group by EryBIV to give TDP-L-mycarose. Although the TDP group may not be the activating nucleotide in all such pathways [5,6], Schulman and coworkers have unambiguously established, by isolation and bioconversion experiments, that avermectin biosynthesis utilizes TDP-L-oleandrose [24]. Its attachment to the avermectin aglycone is catalyzed by the glycosyltransferase AvrB/AveBI while the genes *eryBV* and *tylCV* govern the corresponding steps involving TDP-L-mycarose in the erythromycin [15–18] and tylosin [20] pathways. With this information as a guide, we set out to establish how *avr* genes could be used to convert avermectin aglycones to both known and novel avermectin disaccharides.

2. Results

2.1. Restoration of avermectin production in a S. avermitilis avrCDEFGHI deletion strain

The proposed roles of the *avrBCDEFGHI* genes in avermectin biosynthesis have rested so far mainly on phenotypes of *S. avermitilis* mutants that produce avermectin aglycones only [4,11,12,25,26] and on the relationship of the deduced sequences of the gene products to those of known deoxysugar biosynthesis enzymes [13] (Table 1). The function of AvrE as a TDP-4-keto-2,6-dideoxyhexose reductase has been independently established through the synthesis of 4′-epidaunorubicin and epirubicin [27].

Our first approach involved creating a single plasmid (pWHM482; Fig. 3B) holding the eight genes – *avrBC-DEFGHI* – and introducing it by transformation into *S. avermitilis* GG1657, a strain lacking all the genes of L-oleandrose biosynthesis except *avrB* [9]. The native arrangement of the eight genes [13] suggested that promoters lie between *avrD* and *avrE*, downstream of *avrI* and upstream of *avrB*. Since the latter promoter could be located upstream of the *ORF1* gene adjacent to *avrB* [13] and to ensure expression of *avrB*, a fragment containing the 3′-end of *ORF1* and the genes *avrBCDEFGHI* was excised from pVE1190 [25]. *AvrB* was then orientated downstream of the strong, constitutive *ermE** promoter [28] by cloning it in pWHM1251 [27], a high copy number plasmid derived from the *Escherichia coli*/*Streptomyces* shuttle vector pWHM3 [29]. In the resulting pWHM482 plasmid *avrB* should be expressed under the control of *ermE**p and the seven remaining *avr* genes under that of their native promoters, assuming the cloned fragment indeed contains the *avrI* promoter. (Expression of the avermectin biosynthesis genes in *S. avermitilis* is believed to be controlled, all or in part, by the pathway-specific *avrR* gene located at one end of the gene cluster and encoding a putative DNA-binding protein [13], since deletions or transposon insertions into this region abolish avermectin biosynthesis and bioconversion of avermectin aglycones [9,11,13,25].) *S. avermitilis* GG1657/pWHM482 was grown on solid growth media and the metabolite profile of the strain, analyzed by thin-layer chromatography and high performance liquid chromatography (HPLC) after extraction of

Table 2
Plasmids used in this work

Plasmid	Description
pVE1190	11 kb *Pst*I fragment containing *avrBCDEFGHI* cloned into pVE1053
pWHM465	*Pac*I-*Hin*dIII fragment containing the *act* promoter region cloned from pRM5 into pNEB193
pWHM466	*Fse*I-*Pac*I PCR fragment from pRM5 cloned into pWHM465
pWHM467	*Hin*dIII-*Eco*RI fragment containing *act* promoter region cloned from pWHM466 into pRM5
pWHM468	polylinker LEH3 cloned into pNEB193 between *Eco*RI and *Hin*dIII sites
pWHM469	2.1 kb *Bst*EII-*Kpn*I fragment containing *avrC* and *avrD* cloned from pVE1190 into pWHM468
pWHM470	polylinker LEB4 cloned into pWHM1251 between *Eco*RI and *Bam*HI sites
pWHM471	1.1 kb *Avr*II-*Pst*I fragment containing *avrE* cloned from pWHM470 into pWHM469
pWHM472	1.3 kb *Xba*I-*Avr*II PCR fragment containing *avrB* cloned into pWHM468
pWHM473	1.0 kb *Sst*I-*Pml*I fragment cloned from pVE1190 into pWHM472 to replace central portion of *avrB* amplicon
pWHM474	1.3 kb *Xba*I-*Avr*II fragment containing *avrB* cloned from pWHM473 into pWHM471
pWHM476	1.4 kb *Xho*I-*Nco*I and 2.8 kb *Nco*I-*Not*I fragments from pVE1190, containing *avrF*, *avrG*, *avrH*, and *avrI* were cloned into pANT841
pWHM477	4.2 kb *Bgl*II-*Spe*I fragment containing *avrF*, *avrG*, *avrH*, and *avrI* cloned from pWHM476 into pWHM468
pWHM479	*Xba*I site was eliminated from pWHM474
pWHM480	4.5 kb *Pac*I-*Eco*RI fragment containing *avrB*, *avrE*, *avrD*, and *avrC* cloned from pWHM479 into pWHM467
pWHM481	4.2 kb *Xba*I-*Nsi*I fragment containing *avrI*, *avrH*, *avrG*, and *avrF* cloned from pWHM477 into pWHM480
pWHM482	8.7 kb *Nsi*I-*Hin*dIII fragment containing part of *ORF1* and *avrBCDEFGHI* cloned from pVE1190 into pWHM1250 at the *Pst*I-*Hin*dIII sites
pWHM485	polylinker LSN5 cloned into pGEM-7zf(+) between *Sph*I and *Nsi*I sites
pWHM488	1.25 kb *Spe*I-*Not*I fragment, containing *eryBIII* cloned from pFL401 into pANT841 between *Nhe*I and *Not*I sites
pWHM2100	2.1 kb *Xho*I-*Msc*I fragment cloned from pWHM477 into pSE380
pWHM2101	2.1 kb *Hin*dIII-*Pst*I fragment cloned from pWHM2100 into pWHM468
pWHM2102	pWHM2101 with in-frame deletion in *avrH* gene between *Bpu11021* and *Stu*I sites
pWHM2103	3.1 kb *Sst*I-*Msc*I fragment cloned from pWHM477 into pSE380
pWHM2104	1.4 kb *Msc*I-*Xho*I fragment cloned from pWHM2102 into pWHM2103
pWHM2105	2.4 kb *Msc*I-*Sac*I fragment cloned from pWHM2104 into pWHM477
pWHM2106	3.5 kb *Xba*I-*Nsi*I fragment containing the *avrFGI* and *avrH* with an in-frame deletion cloned from pWHM210 into pWHM480, containing *avrBEDC*
pWHM2107	*Xba*I site was eliminated from pWHM471
pWHM2108	3.25 kb *Pac*I-*Eco*RI fragment cloned from pWHM2107 into pWHM467
pWHM2109	4.2 kb *Xba*I-*Nsi*I fragment containing *avrIHGF* cloned from pWHM477 into pWHM2108, containing *avrEDC*
pWHM2110	In-frame deletion in *avrH* and *avrI* between *Nco*I and *Msc*I sites in pWHM477
pWHM2111	3.2 kb *Xba*I-*Nsi*I fragment containing *avrFG* and *avrHI* with in-frame deletion cloned from pWHM2110 into pWHM480 containing *avrBEDC*
pWHM2129	In-frame deletion in *avrF* in pWHM477 between *Eco*47III and *Sst*I sites
pWHM2130	3.8 kb *Xba*I-*Nsi*I fragment containing *avrF* with in-frame deletion and *avrIHG* cloned from pWHM2129 into pWHM480, containing *avrBEDC*
pWHM2133	3.25 kb *Pml*I-*Nsi*I fragment, containing *avrHGF* and *avrI* with in-frame deletion cloned from pWHM477 into Litmus28
pWHM2134	3.25 kb *Xba*I-*Nsi*I fragment cloned from pWHM2133 into pWHM480, containing *avrBEDC*
pWHM2135	3.25 kb *Xba*I-*Nsi*I fragment cloned from pWHM2133 into pWHM2114, containing *avrBDC*
pWHM2118	1.25 kb *Hin*dIII-*Eco*RI fragment, containing *eryBIII* cloned from pWHM488 into pWHM485
pWHM2119	1.25 kb *Pac*I-*Nsi*I fragment, containing *eryBIII* cloned from pWHM2118 into pKOS025-129
pWHM486	1.55 kb *Spe*I-*Pst*I fragment, containing *eryBV* gene cloned into pANT841
pWHM2120	1.55 kb *Bgl*II-*Pst*I fragment, containing *eryBV* cloned from pWHM486 into Litmus28
pWHM2121	1.55 kb *Xba*I-*Nsi*I fragment, containing *eryBV* cloned from pWHM2120 into pWHM485
pWHM2122	1.55 kb *Pac*I-*Nsi*I fragment, containing *eryBV* cloned from pWHM2121 into pKOS025-129

the plates, proved to be identical to that of the wild-type, avermectin-producing strain *S. avermitilis* MA6593.

2.2. Bioconversion of avermectin A1a aglycone to known avermectins, by recombinant Streptomyces lividans strains hosting plasmid-borne avrBCDEFGHI genes

To avoid working with the rather difficult to transform *S. avermitilis*, our second approach used *S. lividans* as a host for the deoxysugar genes. Avermectin A1a aglycone was exogenously provided within the growth media. The eight *avr* genes were rearranged in two gene cassettes on one plasmid and put under control of the *actI* and *actIII* promoters, respectively. To expedite the cloning work, pRM5 [30] was modified as described in Section 5 to create pWHM467, having new cloning sites introduced downstream of each of the *act* promoters and the *actIII* and *actI–VI* genes of pRM5 deleted. The genes *avrE* and *avrB* first were oriented in the same direction as *avrC* and *avrD* (pWHM480) so that one promoter could control expression of all four of these genes. Genes *avrIHGF* were cloned into pWHM468 (Table 2) having suitable cloning sites to create pWHM477. Next, *avrBEDC* from pWHM480 and *avrIHGF* from pWHM477 were inserted into pWHM467

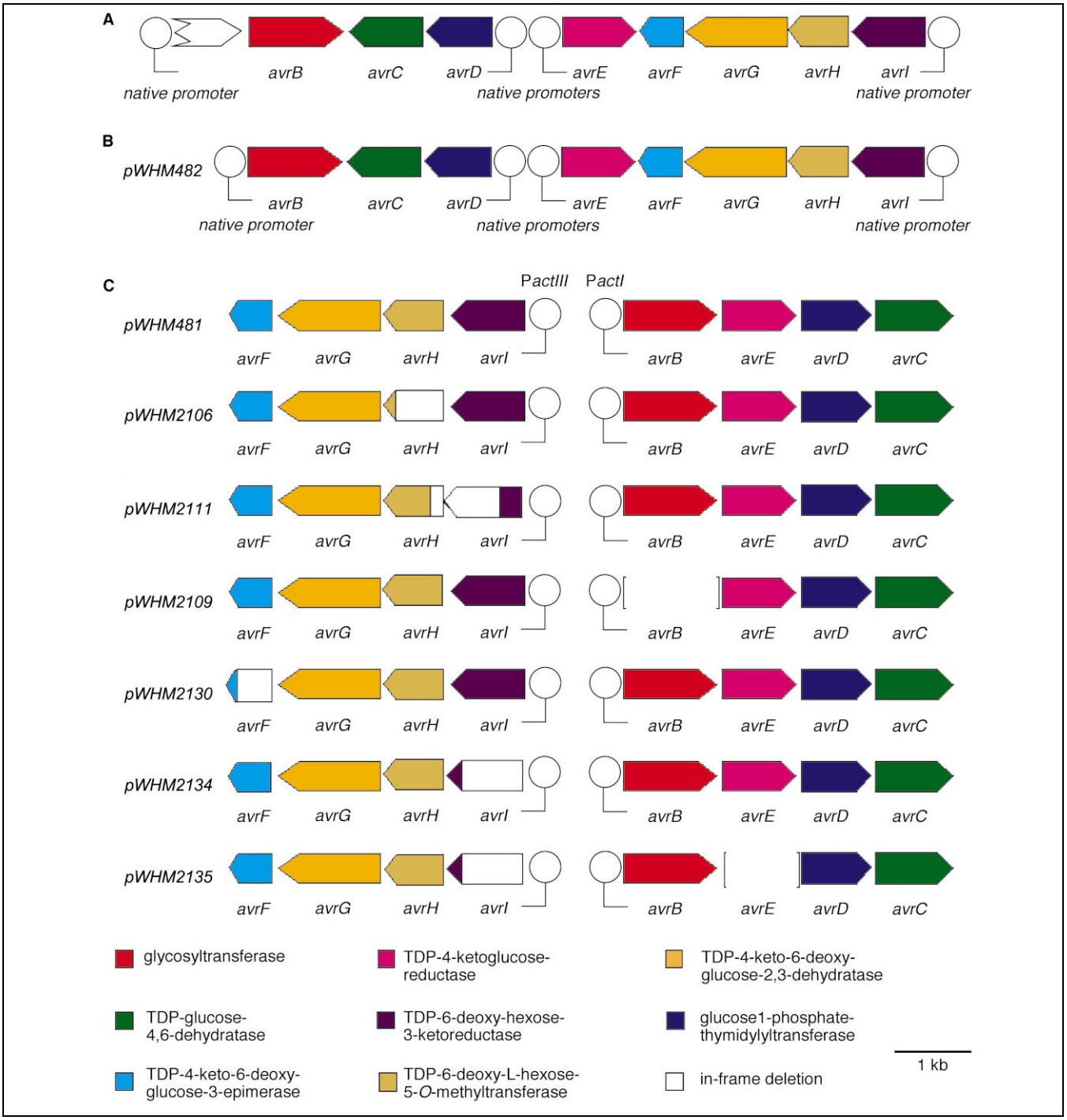

Fig. 3. Constructs for expression of the *avr* L-oleandrose deoxysugar genes. (A) Native arrangement of the *avrBCDEFGHI* genes. (B) and (C) Structure of plasmid-borne constructs with modified versions of *avr* L-oleandrose genes used for biotransformation. Filled wedges oriented in the direction of expression indicate the genes, open brackets indicate the absence of the gene in the construct, and open circles indicate the promoter regions.

downstream of the promoters *actI* and *actIII*, respectively, to create pWHM481 (Fig. 3C), which was transformed into *S. lividans* K4–114 [31].

To verify that *avrB* is essential for formation and transfer of L-oleandrose to the aglycone in avermectin biosynthesis, we created plasmid pWHM2109 (Fig. 3C), hosting genes *avrEDCIHGF* but missing *avrB*. The three genes *avrEDC*, which had already been reoriented all in the same direction, were cloned from plasmid pWHM2107 (Table 2) into pWHM467 before adding the *avrIHGF* cassette in a second step and transforming the resulting plasmid pWHM2109 into *S. lividans* K4–114.

Bioconversion experiments with the *S. lividans* K4–114/pWHM481 and *S. lividans* K4–114/pWHM2109 strains

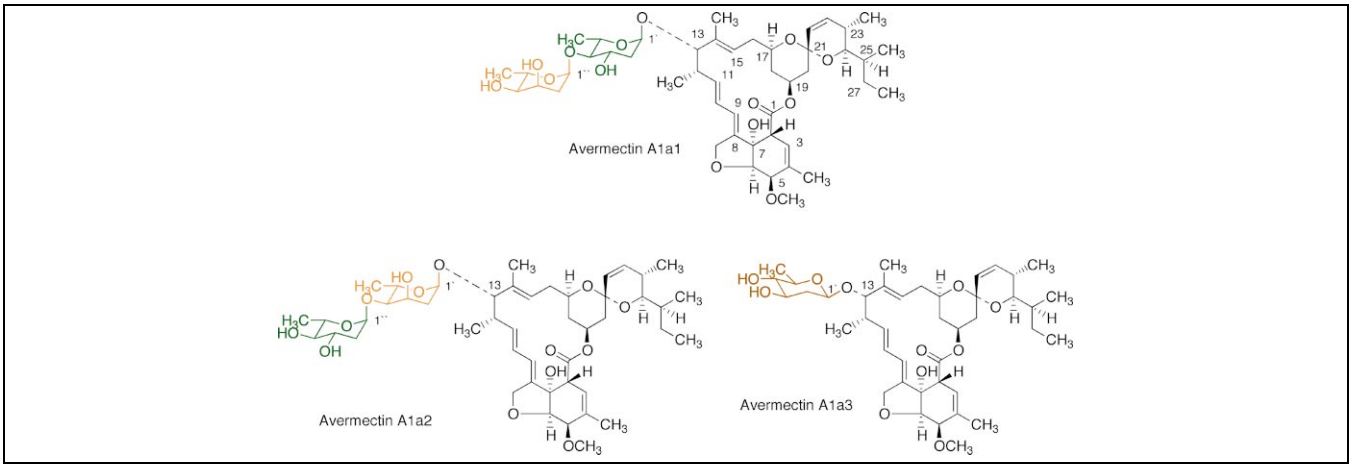

Fig. 4. Novel avermectin A1a derivatives from this work.

were carried out in solid growth media, to which purified avermectin A1a aglycone was added, and the extracts of the strains were analyzed by thin-layer chromatography and HPLC. Fermentation of *S. lividans* K4–114/pWHM481 resulted in the production of avermectin A1a while *S. lividans* K4–114/pWHM2109 did not show conversion of the aglycone. These results, in combination with those gained from the *S. avermitilis* GG1657/pWHM482 strain, confirm that the *avrBCDEFGHI* genes could restore production of TDP-L-oleandrose and support the belief that *avrB* is the glycosyltransferase responsible for attaching the deoxysugar to the avermectin aglycones.

2.3. *Bioconversion experiments to identify the functions of individual avrBCDEFGHI genes*

Our next goal was to take a closer look at the proposed functions of individual genes involved in the biosynthesis of L-oleandrose. For this we wanted to expand our earlier approach using the L-oleandrose genes in two cassettes on a single plasmid by leaving out, deleting, adding or replacing single or multiple genes. By in-frame deletion we eliminated genes from the *avrIHGF* cassette while for manipulation of the *avrBEDC* genes we used cassettes hosting only the genes of interest. The plasmids were transformed

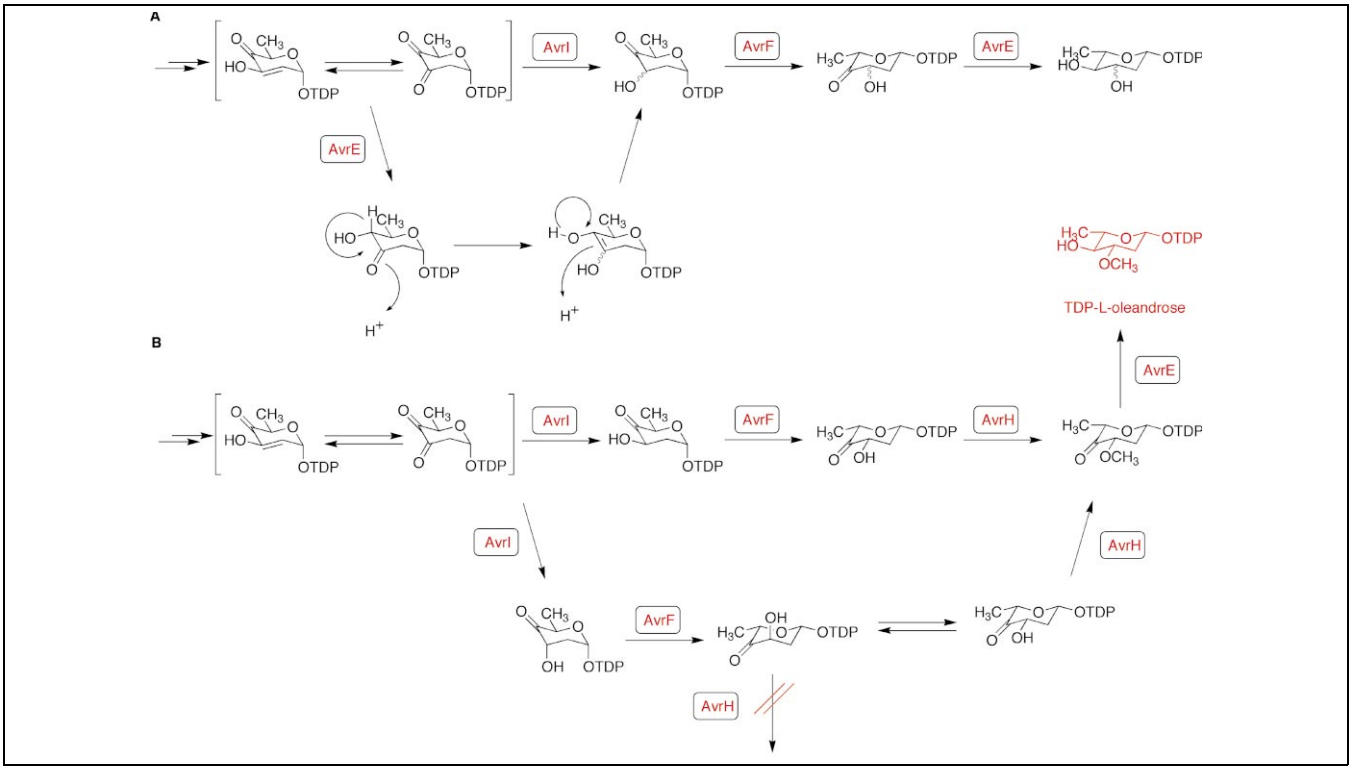

Fig. 5. (A) Hypothesis for substitution of the function of the AvrI 3-ketoreductase by the 4-ketoreductase AvrE and keto-enol tautomerism. (B) A hypothesis for how the AvrH methyltransferase controls the stereochemistry at C-3.

Table 3
Functional assignments for genes associated with the biosynthesis of oleandrose in *S. avermitilis* and mycarose in *S. erythraea*

Plasmid and genes	*m/z*	Possible structures with *m/z* equals $[(M+Na)^+]$; all modifications within the sugar moieties
pWHM482[a], *avrBCDEFGHI*	909.4	avermectin A1a (HPLC confirmed)
	895.5	demethyl-avermectin A1a
	881.5	di-demethyl-avermectin A1a
pWHM481[b], *avrBEDCIIGF*	909.5	avermectin A1a (HPLC confirmed)
	895.5	demethyl-avermectin A1a
	881.5	di-demethyl-avermectin A1a
pWHM2109[b], *avrBEDCIHGF*, Δ*avrB*	–	–
pWHM2106[b], *avrBEDCIGF*, Δ*avrH*	881.5	avermectins A1a1 and A1a2 and at least one more di-demethyl-avermectin A1a
	751.5	desoleandrose-demethyl-avermectin A1a
pWHM2111[b], *avrBEDCGF*, Δ*avrHI*	881.6	avermectins A1a1 and A1a2 (this work) and at least one more di-demethyl-avermectin A1a
	751.6	desoleandrose-demethyl-avermectin A1a
pWHM2134[b], *avrBEDCHGF*, Δ*avrI*	909.6	avermectin A1a (HPLC confirmed)
	895.6	demethyl-avermectin A1a
	893.8	demethyl-4-keto-avermectin A1a
	879.6	demethyl-(demethyl-4-keto)-avermectin A1a
pWHM2130[b], *avrBEDCIHG*, Δ*avrF*	751.6	avermectin A1a3
pWHM2135[b], *avrBDCHGF*, Δ*avrE*Δ*avrI*	909.6	avermectin A1a (HPLC confirmed)
	891.6	demethyl-di-4-keto-avermectin A1a
	877.6	di-demethyl-di-4-keto-avermectin A1a
	763.6	desoleandrose-4-keto-avermectin A1a
	749.6	desoleandrose-(demethyl-4-keto)-avermectin A1a
pWHM2106+pWHM2119[b], *avrBEDCIGF*, *avr*Δ*H*+*eryBIII*	895.6	di-demethyl-3′/3″-*C*-methyl-avermectin A1a
	881.6	di-demethyl-avermectin A1a
	879.6	demethyl-(demethyl-4-keto)-avermectin A1a
	751.6	desoleandrose-demethyl-avermectin A1a

–, no bioconversion observed and therefore also no mass data.
[a]Carried in *S. avermitilis* GG1657.
[b]Carried in *S. lividans* K4–114.

into *S. lividans* K4–114 and once again grown on aglycone-enriched solid media to trap any produced deoxysugars in avermectin A1a glycosides.

In a first experiment we investigated AvrH, supposed to be a 3-*O*-methyltransferase. Fermentation of *S. lividans* K4–114/pWHM2106 (Δ*avrH*; Fig. 3C), which contains only the genes *avrIGF* and *avrBEDC*, in the presence of avermectin A1a aglycone led to a number of products with UV-absorption pattern typical for avermectins. Analytical and semi-preparative HPLC followed by mass spectrometry showed that no avermectin A1a was produced but indicated the formation of avermectin A1a derivatives having demethylated mono- and disaccharide moieties (Table 3). With a conversion rate of less than 5% we concentrated on isolating only the main products and were able to characterize the two novel disaccharide avermectins A1a1 and A1a2 (Fig. 4) by mass spectrometry as well as one- and two-dimensional (1D and 2D) proton and carbon nuclear magnetic resonance (NMR) spectroscopy. A third avermectin derivative, having the same mass as the avermectins A1a1 and A1a2, was also isolated but not characterized. The carbon spectra of both compounds showed 47 signals. Chemical shifts and couplings observed in the H,H-COSY, HSQC and HMBC spectra confirmed the structure of the aglycone to be that of avermectin A1a, accounting for 35 carbon signals. For each compound two anomeric proton signals were identified and using the 2D-NMR spectra a total of six carbon signals could be assigned for each of the sugars. Small coupling constants (3.4, 0.8 and 4.1, 1.0 Hz, respectively) confirmed that both were sugars of the L-series and α-glycosidically linked. Deoxygenated methylene groups were assigned for position 2 of each sugar and CH groups for positions 3, 4 and 5, followed by a 6-methyl group. The coupling patterns and constants for the proton signals at C-2, C-3 and C-4 facilitated the assignment of the configuration for each deoxysugar and compound as shown in Fig. 4. The patterns of the 4-H were particularly helpful; two large axial–axial couplings (around 9 Hz) indicated two axial protons in close proximity (3-H and 5-H) while a large axial–axial and a smaller equatorial–axial one indicated axial (5-H) and equatorial (3-H) neighboring protons. 1D-TOCSY and 1D-NOESY NMR verified the configuration of 3-H of the deoxysugars. The interconnectivities between sugar–aglycone and sugar–sugar were determined for avermectin A1a1 by couplings observed in the HMBC and 2D-NOESY spectrum. For avermectin A1a2 the sugar–sugar connection was concluded from the 2D-NOESY spectrum while the interglycosidic linkage followed from the chemical shifts. The structures of the two compounds

showed that the hydroxyl groups in position 3 of the deoxysugars in both cases had not been methylated, confirming that *avrH* encodes a 3-*O*-methyltransferase. Avermectin A1a1 has L-olivose (demethylated L-oleandrose) attached to the aglycone, followed by a 2,6-dideoxy-L-ribo-hexopyranose (L-digitoxose) that structurally differs from L-olivose in its inverted configuration of the C-3 stereocenter. In avermectin A1a2 this sugar is directly attached to the aglycone, with L-olivose completing the disaccharide moiety (Fig. 4).

For a second and third experiment we created plasmids hosting the genes *avrBEDCHGF* (pWHM2134; Δ*avrI*) and *avrBEDCGF* (pWHM2111; Δ*avrHI*), respectively. pWHM2134 is missing the *avrI* 3-ketoreductase gene supposed to be involved in the 2-deoxygenation of the deoxysugar, while pWHM2111 has the genes encoding the 3-ketoreductase and the 3-*O*-methyltransferase disrupted (Fig. 3C). HPLC analysis and mass spectrometry of the metabolites produced by *S. lividans* K4–114/pWHM2134 showed that avermectin A1a was still being made as well as avermectin A1a derivatives with mono- or di-demethylated disaccharides (Table 3). *S. lividans* K4–114/pWHM2111 (Δ*avrHI*) gave the same overall metabolic profile as *S. lividans* K4–114/pWHM2106 (Δ*avrH*), producing avermectins A1a1 and A1a2. These results, which mirror those observed for the L-mycarose pathway in *Saccharopolyspora erythraea* [18], let us conclude that the function of AvrI as a 3-ketoreductase in the 2-deoxygenation steps of the deoxysugar biosynthesis can be either replaced by a similar ketoreductase from *S. lividans* or be substituted by the 4-ketoreductase AvrE after keto-enol tautomerism (Fig. 5A). In the proposed pathway the 3-keto group caused by the 2-deoxygenation would be reduced by the AvrI 3-ketoreductase, followed by epimerisation, methyl transfer and finally the reduction of the 4-keto group by AvrE. However, the 3-keto group could, by keto-enol tautomerism, be moved into the 4-position. Reduction of the 4-keto group by AvrE would now make the AvrI 3-ketoreductase redundant.

To take a closer look at the epimerization step that is responsible for switching from the D- into the L-series of sugars in this pathway, we constructed pWHM2130, having the proposed epimerase gene *avrF* removed by in-frame deletion (Fig. 3C). HPLC analysis of the fermentation extracts of *S. lividans* K4–114/pWHM2130 showed only one compound with a typical avermectin UV-absorption spectrum. Mass spectrometry data indicated an avermectin with a demethylated monosaccharide moiety and by 1D- and 2D-NMR the compound was characterized to be avermectin A1a3, with D-olivose as the deoxysugar (Fig. 4). Thirty-five of the 41 carbon signals observed could again be assigned to the avermectin A1a aglycone. The deoxysugar protons 3, 4 and 5 were all observed to be in axial configuration, while the larger axial–axial and smaller equatorial–axial coupling pattern for the single anomeric proton (10.0 and 1.7 Hz), caused by the neighboring methylene group, proved this sugar to be D-olivose, β-glycosidically linked to the aglycone. The only alternative structure for a deoxysugar having the same characteristic signals and patterns would have been L-olivose, also β-glycosidically connected. However, this would raise the question why L-olivose should have been linked β-glycosidically here when L-sugars in nature are normally found to be linked α-glycosidically. Avermectins A1a1 and A1a2 (Fig. 4) have L-olivose α-glycosidically connected to the aglycone. Having D-olivose attached to the aglycone proves that AvrF is indeed the epimerase of the L-oleandrose biosynthetic pathway, but acts as a 5- and not a 3,5-epimerase, as explained further below. The attachment of D-olivose instead of L-oleandrose to the aglycone also shows that the AvrB glycosyltransferase is relatively flexible towards its deoxysugar substrates, as has already been observed for a number of glycosyltransferases from other pathways [32–38]. In our case, this flexibility finds a limit in the inability to interconnect two D-olivose molecules, which confirms the report by Schulman et al. [24] that two monosaccharides and not a disaccharide are transferred consecutively to the avermectin aglycone.

An interesting aspect of avermectin A1a3 is the equatorial *R*-configuration of the C-4′ stereocenter of D-olivose. In the native biosynthetic pathway AvrE, the 4-ketoreductase, is thought to catalyze the last step before attaching the sugar to the aglycone, which creates the equatorial *S*-configuration at position 4 as in avermectin A1a (Fig. 1). This can be explained in two ways: (i) AvrE is rather flexible, having its 4-keto sugar substrate located in such a way that the resulting 4-hydroxyl group is always found in an equatorial configuration. (ii) AvrE is not flexible and a 4-ketoreductase from *S. lividans* substitutes for AvrE, reducing the 4-keto group into the configuration found.

Although we do not have conclusive support for either hypothesis we favor explanation (ii), since the AvrB glycosyltransferase seems to tolerate both equatorial and axial hydroxyl groups in position 3 (see avermectins A1a1 and A1a2). We found only avermectin A1a3 but no avermectin glycosylated with D-oliose (β-D-oliose differs from D-olivose and D-oleandrose by having the 4-hydroxyl group in the axial instead of equatorial position). This may indicate that the flexibility of AvrB is limited to only the three positions in L-deoxysugars. However, in another experiment where we removed both *avrI* and *avrE* from our eight-member gene set (plasmid pWHM2135; Fig. 3C), HPLC and mass spectrometry analysis of fermentation extracts from *S. lividans* K4–114/pWHM2135 indicated the production of several derivatives with methylated and demethylated mono- and disaccharides attached to the avermectin A1a aglycone (Table 5). These compounds were not further characterized due to low conversion rates. We also observed production of avermectin A1a in low yield. These results show that the functions of AvrE and AvrI can be substituted by

similar enzymes from *S. lividans*, as already observed for a related pathway [18].

Further information about how the stereochemistry at C-3 in the L-oleandrose pathway is controlled and the function of the AvrF epimerase comes from some of our earlier experiments above. Both the Δ*avrH* and Δ*avrHI* mutant strains produced avermectins having sugar moieties with a 3-*R*- or 3-*S*-configuration, respectively. The AvrE 4-ketoreductase and the AvrF epimerase were still present in both cases. Tight control by either AvrI or AvrF over the C-3 stereochemistry should have resulted in deoxysugars with 3-*S*-configuration only and not a mixture of C-3 isomers as observed. This implies that the AvrH methyltransferase only methylates an equatorial hydroxyl group at C-3. In the normal pathway any deoxysugar intermediates with initially axial C-3 hydroxyl groups would not be methylated until keto-enol tautomerism causes isomerisation of the hydroxyl group (Fig. 5B). This idea also does not contradict the fact that avermectin A1a3 is the only product of *S. lividans* K4–114/pWHM2130 (Δ*avrF*) without traces of a second (or more) products having the corresponding D-sugar with an axial instead of an equatorial hydroxyl group at C-3. Our data show that the AvrB glycosyltransferase has a limited ability to handle D-deoxysugars and might not be able to attach two D-sugars to the aglycone.

We conclude from these results that, regardless of the actual sequence of individual steps in the deoxysugar pathway, the configuration of C-3 is ultimately determined by the AvrH methyltransferase and not by the AvrF epimerase nor the AvrI 3-ketoreductase. The results also show that AvrF is a 5-epimerase and not a 3,5-epimerase.

2.4. *Bioconversion of avermectin A1a aglycone to novel avermectins by combining genes from different deoxysugar biosynthetic pathways in S. lividans*

The above results show that different deoxysugars can be attached to the avermectin A1a aglycone by modifying the biosynthesis of L-oleandrose. We next wanted to extend this approach by combining different deoxysugar pathways with one another. We decided to combine the *avr* genes with *eryB* genes from the closely related mycarose pathway of erythromycin biosynthesis in *S. erythraea*. The proposed 3-*C*-methyltransferase encoded by *eryBIII* was chosen for our initial experiments.

Co-transformation of *S. lividans* K4–114 with plasmids pWHM2106 (*avrBEDCIGF*, Δ*avrH*) and pWHM2119 (*eryBIII*; Table 2) could potentially lead to an avermectin A1a derivative having one or two L-mycarose molecules attached. A bioconversion experiment with the resulting strain gave only very low conversion rates (around 0.1%) to what appeared to be glycosylated avermectin compounds. We did not isolate sufficient amounts of any of these metabolites for NMR analysis, but mass spectrometry data indicated the production of an avermectin derivative with two 2,6-dideoxyhexoses, both bearing additional methyl groups. Since we knew from our earlier experiment that the gene for the 3-*O*-methyltransferase, *avrH*, had been successfully disrupted in plasmid pWHM2106, any additional methyl groups had to result from a 3-*C*-methyltransferase by EryBIII. Therefore, the result is consistent with the successful combination of *avr* and *eryBIII* genes.

3. Discussion

We have examined the possibilities of using single and dual plasmid systems for expression of deoxysugar biosynthesis genes in a heterologous host to both verify the function of genes that had been assigned on the basis of sequence analysis and to produce novel avermectin glycosides. The 2,6-dideoxysugar L-oleandrose was chosen for our experiments as the individual steps in its biosynthesis are predictable and the rearrangement of the eight genes involved in its biosynthesis into two gene cassettes offered a convenient way to construct various expression plasmids. The inherent risk is that changes in gene expression caused by reorganization of some of the *avrBCDEFGHI* genes into artificial operons, or effects of the heterologous host on enzyme activity, would result in low product yields in the bioconversion experiments. Nonetheless, the results obtained prove that the approach, which builds upon our recent study of the formation anthracycline glycosides by the same method [39], is overall a useful way to produce both known and novel glycosides.

We were able to both restore avermectin production in a *S. avermitilis* mutant missing all genes required for the biosynthesis of L-oleandrose and produce avermectin A1a in *S. lividans* using exogenously supplied aglycone. Modifications of the plasmid-borne *avr* genes also enabled us to verify and decode the function of several individual steps and enzymes in the biosynthesis of L-oleandrose, and led to the production of three novel avermectins, including the first avermectin with a D-deoxysugar attached to its aglycone. (Although rare, there are at least two other reports where glycosyltransferases recognize both D- and L-deoxysugars [34,38].) Our results confirm that AvrH is the 3-*O*-methyltransferase of the L-oleandrose biosynthetic pathway and ultimately determines the configuration of the C-3 stereocenter. AvrF was shown to be not a 3,5- but a 5-epimerase only. On the basis that AvrE and AvrI are indeed (3- and 4-)ketoreductases, respectively, as predicted by gene sequence homologies, we further conclude that similar enzymes from *S. lividans* can substitute for these two enzymes.

The results also suggest a degree of both substrate flexibility and inflexibility for the AvrB glycosyltransferase. AvrB seems to attach and interconnect deoxysugars that differ from its natural substrate by missing the 3-*O*-methyl group, having inverted configuration at the C-3 stereocen-

ter, and probably a 3-*C*- instead of a 3-*O*-methyl group. This glycosyltransferase can also attach D-olivose to the avermectin aglycone, but is unable to interconnect two D-monosaccharides. This result shows that AvrB transfers a monosaccharide substrate to the aglycone in two consecutive steps instead of a single disaccharide.

4. Significance

Combinatorial biosynthesis to gain new natural products is greatly expedited when the novel gene combinations or deletions can be rapidly constructed in vitro and evaluated in vivo. This has been most efficiently achieved by using plasmid vectors and an easily transformable host in which the introduced genes are well expressed. McDaniel et al. [40] and Xue et al. [41] have recently demonstrated the power of this approach, using modular polyketide synthase genes. Deoxysugar biosynthesis genes are equally suitable, as demonstrated by the macrolide antibiotics [33,35,36], the angucyclines and tetracenomycins [32,34,37], glycopeptide antibiotics [42], and the anthracycline epirubicin [27]. Many of these studies have depended on the construction of a mutation in one or more deoxysugar biosynthesis genes located in the chromosome of the producing organism, followed by creation of the novel gene combination through introduction of a plasmid-borne gene or a gene replacement experiment. Such work is time consuming and often thwarted when the host is difficult to transform. Our method, as described here and earlier [39], avoids some of these problems and is amenable to creating a large library of recombinants that can be screened for variations in the biological activity of known glycosides, or for the formation of novel glycosides by the bioconversion of a library of aglycones. The limitation of the glycosyltransferase flexibility or specificity towards either the aglycone and TDP-deoxysugar substrate might be possible to overcome by efficient mutagenesis of glycosyltransferase genes using DNA shuffling and other methods [43].

5. Materials and methods

5.1. Bacterial strains and plasmids

E. coli strain DH5α [44] and plasmids pNEB193 and Litmus28 (New England Biolabs) and pANT841, a pUC19 derivative with additional cloning sites (C. DeSanti, Ohio State University), pSE380 (Invitrogen), pGEM-7zf(+) (Promega) and pVE1053 [45] were used for routine subcloning. The L-oleandrose biosynthetic genes from *S. avermitilis* are located on pVE1190 (D. MacNeil, Merck and Co.). The pWHM1251 plasmid containing *avrE* was from an earlier study [27]. Low copy number shuttle vector pRM5 containing the dual *act* promoter system [30] as well as pRM5 derivative pKOS025-129 carrying a hygromycin resistance marker [41], pFL401 containing *eryBIII* gene, and the *S. lividans* K4–114 strain containing a chromosomal deletion of the entire actinorhodin gene cluster [31] were from Kosan Biosciences. *S. avermitilis* Δ1066 strain was used in which all the oleandrose genes but *avrB* were deleted [9]. Plasmids used in this study are listed in Table 2.

5.2. Media and growth conditions

S. lividans K4–114 was maintained on R2YE agar [46] without

Table 4
^{13}C NMR data of the novel avermectins A1a1, A1a2, A1a3 (relative to TMS, * in methanol-d_4, # in chloroform-d_1, 125.9 MHz, δ, multiplicity (DEPT))

	A1a1*	A1a2*	A1a2#	A1a3*
1	173.0, s	173.0, s	173.0, s	173.8, s
2	46.8, d	46.8, d	45.6, d	46.9, d
3	121.3, d	121.3, d	118.3, d	121.2, d
4	134.5, s	134.8, s	136.0, s	135.2, s
4a	19.9, q	19.9, q	19.9, q	19.9, q
5	78.3, d	78.3, d	77.9, d	78.2, d
5a	57.8, q	57.7, q	57.8, q	55.7, q
6	79.4, d	79.4, d	78.0, d	79.4, d
7	83.0, s	82.0, s	80.5, s	81.1, s
8	141.0, s	141.0, s	140.5, s	141.2, s
8a	68.7, t	68.7, t	68.0, t	68.7, t
9	121.8, d	121.8, d	119.5, d	121.8, d
10	126.5, d	126.4, d	125.5, d	126.2, d
11	138.5, d	138.4, d	136.4, d	139.0, d
12	41.0, d	41.0, d	39.5, d	40.9, d
12a	20.9, q	20.6, q	20.3, q	20.0, q
13	83.9, d	83.5, d	82.0, d	84.0, d
14	136.5, s	136.6, s	134.5, s	137.2, s
14a	15.2, q	15.1, q	15.1, q	15.0, q
15	119.8, d	119.6, d	119.4, d	119.2, d
16	35.0, t	35.1, t	34.3, t	35.1, t
17	70.2, d	70.0, d	68.0, d	70.1, d
18	37.6, t	37.6, t	36.6, t	37.5, t
19	70.0, d	69.8, d	68.0, d	69.9, d
20	42.0, t	42.0, t	40.5, t	42.0, t
21	97.3, s	97.3, s	95.8, s	97.3, s
22	136.5, d	136.5, d	136.3, d	136.6, d
23	129.3, d	129.3, d	127.8, d	129.2, d
24	31.8, d	31.8, d	30.6, d	31.8, d
24a	16.8, q	16.8, q	16.4, q	16.8, q
25	75.9, d	75.9, d	74.8, d	75.9, d
26	36.5, d	36.5, d	35.3, d	36.6, d
26a	13.5, q	13.5, q	13.0, q	13.5, q
27	28.6, t	28.6, t	27.5, t	28.5, t
28	12.6, q	12.5, q	12.1, q	12.5, q
1′	96.2, d	95.9, d	95.0, d	99.1, d
2′	39.5, t	36.1, t	35.2, t	40.8, t
3′	70.3, d	63.6, d	62.7, d	72.5, d
4′	84.3, d	76.6, d	75.1, d	78.7, d
5′	68.7, d	64.3, d	62.7, d	73.2, d
6′	18.7, q	18.1, q	18.2, q	17.2, q
1″	99.4, d	94.3, d	92.4, d	–
2″	36.2, t	38.9, t	37.7, t	–
3″	68.2, d	69.7, d	69.3, d	–
4″	74.1, d	78.8, d	78.4, d	–
5″	65.9, d	69.8, d	68.0, d	–
6″	18.1, q	18.6, q	17.6, q	–

Table 5
^{1}H NMR data of the novel avermectins A1a1, A1a2, A1a3 (relative to TMS, * in methanol-d_4, # in chloroform-d_1, 500.6 MHz, δ)

	A1a1*	A1a2*	A1a2#	A1a3*
2	3.22, m	3.22, m	3.31, m	3.21, m
3	5.47, m	5.47, m	5.38, m	5.47, m
4a	1.79, s	1.78, s	1.81, s	1.78, s
5	3.95[a], m	3.93[a], m	3.98, m	3.89[a], m
5a	3.46, s	3.46, s	3.50, s	3.46, s
6	3.95[a], m	3.93[a], m	4.03, m	3.89[a], m
8a	4.61, dd, 14.3, 2.2	4.62, dd, 14.4, 2.3	4.62, dd, 14.6, 2.1	4.60, dd, 14.5, 2.1
	4.65, dd, 14.3, 2.2	4.64, dd, 14.4, 2.3	4.64, dd, 14.6, 2.1	4.64, dd, 14.5, 2.1
9	5.82, ddd, 11.3, 2.2, 2.2	5.82, ddd, 11.1, 2.3, 2.3	5.81, ddd, 11.0, 2.1, 2.1	5.80, ddd, 11.2, 2.1, 2.1
10	5.89, dd, 14.8, 11.3	5.89, dd, 14.9, 11.1	5.76, dd, 14.1, 11.0	5.86, dd, 14.5, 11.2
11	5.72, dd, 14.8, 9.8	5.79, dd, 14.9, 9.8	5.62, dd, 14.1, 9.8	5.65, dd, 14.5, 9.9
12	2.65, ddq, 9.8, 6.9, 2.5	2.65, ddq, 9.8, 6.9, 2.9	2.65, ddq, 9.8, 6.9, 2.9	2.60, ddq, 9.9, 6.8, 3.1
12a	1.16, d, 6.9	1.20, d, 6.9	1.20, d, 6.9	1.12, d, 6.8
13	3.99, s br	4.05, s br	4.05, s br	4.09, s br
14a	1.54, s	1.54, s	1.51, s	1.53, s
15	5.15, dd, 8.0, 4.9	5.22, dd, 9.0, 4.7	5.05, dd, 10.4, 4.7	5.24, dd, 10.7, 4.4
16	2.27, m	2.28, m	2.29, m	2.26, m
17	3.89, m	3.89, m	3.86, m	3.89, m
18e	1.93, ddd, 14.3, 4.2, 4.2	1.96, m	1.74, m	1.92, ddd, 12.7, 4.5, 4.5
18a	0.85, m	0.84, m	0.88, m	0.86, m
19	5.05, dddd, 11.3, 11.3, 4.2, 4.2	5.05, dddd, 11.2, 11.2, 4.6, 4.6	5.36, m	5.04, dddd, 11.8, 11.8, 4.5, 4.5
20e	2.20, ddd, 12.0, 4.2, 1.1	2.17, m	2.03, ddd, 12.0, 4.7, 1.6	2.19, ddd, 11.8, 4.5, 1.6
20a	1.36, m	1.35, m	1.48, m	1.35, m
22	5.75, dd, 10.0, 1.4	5.74, dd, 9.9, 1.7	5.77, dd, 10.0, 1.6	5.75, dd, 10.0, 1.6
23	5.54, dd, 10.0, 2.6	5.54, dd, 9.9, 2.6	5.55, dd, 10.0, 2.7	5.54, dd, 10.0, 2.5
24	2.29, m	2.29, m	2.28, m	2.29, m
24a	0.92, d, 7.2	0.92, d, 7.4	0.91, d, 6.9	0.92, d, 7.2
25	3.48, m	3.48, m	3.47, m	3.46, m
26	1.63, m	1.63, m	1.60, m	1.65, m
26a	0.94, d, 7.0	0.94, d, 6.9	0.93, d, 7.3	0.94, d, 6.7
27	1.48–1.54, m	1.47–1.54, m	1.48–1.54, m	1.48–1.58, m
28	0.98, t, 7.1	0.98, t, 7.4	0.95, t, 7.1	0.99, t, 7.3
1′	4.75, dd, 3.4, 0.8	4.75, dd, 3.5, 0.9	4.83, dd, 3.4, 0.8	4.38, dd, 10.0, 1.7
2′e	2.08, ddd, 12.9, 5.0, 0.8	2.15, m	2.14, ddd, 14.3, 3.2, 0.8	2.14, ddd, 12.1, 5.2, 1.7
2′a	1.70, m	1.98, ddd, 14.7, 3.5, 3.5	1.92, ddd, 14.3, 3.4, 3.2	1.60, m
3′	4.02, m	4.25, m	4.27, ddd, 3.2, 3.2, 2.9	3.48, m
4′	3.12, dd, 9.0, 9.0	3.30[b]	3.29, dd, 9.0, 2.9	2.91, dd, 9.0, 9.0
5′	3.89, dq, 9.0, 6.2	4.29, dq, 9.1, 6.2	4.19, dq, 9.0, 6.4	3.14, dq, 9.0, 6.2
6′	1.28, d, 6.2	1.23, d, 6.2	1.27, d, 6.4	1.26, d, 6.2
1″	5.28, dd, 4.1, 1.0	5.10, dd, 4.0, 0.9	5.18, dd, 3.7, 0.8	–
2″e	2.21, m	2.18, ddd, 14.2, 11.2, 4.0	2.23, ddd, 13.1, 5.0, 0.8	–
2″a	1.93, m	1.62, ddd, 14.2, 5.1, 0.9	1.71, m	–
3″	3.94, m	3.79, ddd, 11.2, 9.1, 5.1	3.95, m	–
4″	3.19, dd, 9.2, 3.2	2.95, dd, 9.1, 9.1	3.19, dd, 9.2, 9.2	–
5″	4.08, dq, 9.2, 6.2	3.65, dq, 9.1, 6.2	3.67, dd, 9.2, 6.4	–
6″	1.23, d, 6.2	1.24, d, 6.2	1.30, d, 6.4	–

[a]Assignment interchangeable.
[b]Only indirectly observed in 2D experiments due to overlapping with solvent.

sucrose and grown in liquid R2YE for preparation of protoplasts and seed inoculums. Protoplasts were regenerated on R2YE agar with thiostrepton (obtained from S.L. Lucania, Bristol-Myers-Squibb, Princeton, NJ, USA) or hygromycin selection at 30 μg/ml and 200 μg/ml in solid medium and 5 μg/ml and 55 μg/ml for liquid medium correspondingly. The *E. coli* strains were grown in LB medium [44] supplemented with ampicillin (100 μg/ml) for selection of plasmids.

5.3. DNA isolation and in vitro manipulation

Plasmid DNA was isolated from bacterial cells with the Bio 101 Kit (Vista, CA, USA) or by standard procedures [44]. Restriction endonuclease digestion and ligation was performed using standard techniques [44]. DNA fragments for subcloning were isolated with the Qiaex (Qiagen) gel extraction kit or by phenol: chloroform extraction [44] from SeaPlaque low melting agarose

(FMC Bioproducts, Rockland, ME, USA). Sequencing reactions using reverse and forward M13 primers were performed with an ABI Prism Big Dye terminator cycle sequencing kit at the University of Wisconsin Biotechnology Center. To introduce unique *Fse*I, *Nsi*I, and *Xba*I restriction sites downstream of the *actIII* promoter in pRM5, two oligonucleotides, PM1 and PO2, were designed for replacement of the original plasmid DNA. The sequence of the original and new DNA is as follows. Original DNA: 5′-TCCTGCGTGGCCATGTGTTCCctccCTGCCTCG-TGGTCC-3′; PM1: 5′-TCCTG***GCC***GGCCATG***CA***TTCCctcc-CTG***T***CT***A***G***A***GGTCC-3′. Changes are shown in bold italic with the *actIII* ribosome-binding site (rbs) in lower case. The second oligonucleotide, PO2, was distal to the *Pac*I site in pRM5 downstream of the left promoter to allow *Pac*I digestion of the PCR product. The sequence of this primer was identical to that of pRM5: 5′-CCCAGTCACGACGTTGTAAAACGACGGCC-3′.

A new polylinker, LEH3, for pNEB193 was created as a synthetic oligonucleotide containing rbs and the following internal sites: *Bst*EII, *Kpn*I, *Pst*I, *Avr*II, *Xba*I, *Pac*I, *Bgl*II, *Spe*I, *Nsi*I. Top strand: 5′-AATTCGGTAACCGGTACCCTGCAGCCTA-GGTCTAGAGGAGGATTAATTAAAGATCTACTAGTATG-CATA-3′; bottom strand: 3′-GCCATTGGCCATGGGAC-GTCGGATCCAGATCTCCTCCTAATTAATTTCTAGATGA-TCATACGTATTCGA-5′. The LEH3 polylinker was used to replace the original polylinker of pNEB193 by cloning into the *Eco*RI and *Hin*dIII sites to create pWHM468. Similarly, a synthetic DNA linker, LEB4, containing rbs and the internal sites *Xba*I and *Avr*II were cloned between the *Eco*RI and *Bam*HI sites of the polylinker of pWHM1251 to create pWHM472; top strand: 5′-AATTCTCTAGACCTAGGGGAGGAG-3′; bottom strand: 3′-GAGATCTGGATCCCCTCCTCCTAG-5′. A new polylinker, LSN5, for pGEM-7zf(+) was created as a synthetic oligonucleotide containing rbs and the following internal sites: *Pac*I, *Hin*dIII, *Msc*I, *Eco*RI, *Xba*I, *Bgl*II, and *Pst*I. Top strand: 5′-CTTAATTAAGGAGGAAAGCTTTGGCCAGAATTCTCT-AGAAGATCTCTGCAGATGCA-3′; bottom strand: 3′-GT-ACGAATTAATTCCTCCTTTCGAAACCGGTCTTAAGAGA-TCTTCTAGAGACGTCT-5′. The LSN5 polylinker was used to replace the original polylinker of pGEM-7zf(+) by cloning into *Sph*I and *Nsi*I sites to create pWHM485.

To create plasmid pWHM472 a 1.3 kb PCR amplicon for *avrB* with *Xba*I-*Avr*II sites was made (Easy Start Kit, Molecular Bio-Products, Inc.). The following two primers were used: PO6: 5′-TTTTCTAGACAGTGAGAGATGTCAGATCA-3′ and PO7: 5′-TTTCCTAGGAACCCTGTGGGAGCCACTCA-3′ to introduce the needed *Xba*I and *Avr*II sites. Amplification was made using the Easy Start Kit. The reaction mixture was incubated at 94°C for 2 min and then 30 cycles of denaturing (94°C, 1 min), annealing (55°C, 1.5 min) and elongation (70°C, 2 min) followed by a cycle of elongation (70°C, 10 min).

5.4. Modification of vector pRM5 for in vivo expression of avermectin L-oleandrose genes

The shuttle vector pRM5 has been used for expressing polyketide synthase genes in *Streptomyces coelicolor* strains that lack the entire *act* biosynthetic cluster [30]. To make this vector more useful for cloning and expression of *Streptomyces* genes, the following modifications were done as described below: (a) part of *actIII* was deleted to ensure that the ActIII protein would not be expressed, (b) the *act* genes downstream of the *actI* promoter were deleted, and (c) new cloning sites were introduced downstream of both the *actI* and *actIII* promoters. The *Hin*dIII-*Pac*I fragment containing the *actI*/*actIII* promoter region was cloned into pNEB193 to facilitate manipulation and to provide an *Eco*RI site next to the *Pac*I site (pWHM465, Table 2). A PCR fragment was amplified using primers PM1 and PO2 (above) to introduce unique *Fse*I, *Nsi*I, and *Xba*I sites downstream of the *actIII* promoter. The new *Fse*I site allowed the deletion of about one-third of *actIII* by cutting a single internal *Fse*I site followed by religation. The PCR product was digested with *Fse*I and *Pac*I and cloned into pWHM465 to yield pWHM466 (Table 2). The *Hin*dIII-*Eco*RI fragment from pWHM466 containing the *actII*-ORF4 activator gene and *act* promoter region was used to replace the *act* genes in pRM5 to give pWHM467. Amplification was made as described above.

Table 6
HMBC couplings of avermectin A1a1 in methanol-d_4 (δ, relative to TMS)

Position	^{1}H	^{13}C	Position
4a	1.79	78.3	5/6
		121.3	3
		134.5	4
5a	3.46	78.3	5/6
5/6	3.95	46.8	2
12a	1.16	41.0	12
		83.9	13
		138.5	11
14a	1.54	83.9	13
		119.8	15
		136.4	14
18a	0.85	70.2	17
24a	0.92	31.8	24
		75.9	25
		136.5	22
26a	0.94	28.6	27
		36.5	26
		75.9	25
28	0.98	36.5	26
		28.6	27
4′	3.12	68.7	5′
		99.4	1″
6′	1.28	84.3	4′
		68.7	5′
2″a	1.93	68.2	3″
4″	3.19	65.9	5″
6″	1.23	74.1	4″
		65.9	5″

5.5. Construction of plasmids for expression of the avrBCDEFGHI genes

Plasmid pWHM482 was constructed using the *Streptomyces* expression vector pWHM1250 and the native L-oleandrose bio-

Table 7
H,H-COSY couplings of avermectin A1a1 in methanol-d_4 (δ, relative to TMS)

Position	^{1}H	^{1}H	Position
2	3.22	1.79	4a
		3.95	5/6
		5.47	3
3	5.47	1.79	4a
		3.22	2
		3.95	5/6
4a	1.79	3.22	2
		5.47	3
5/6	3.95	5.47	3
6	3.95	3.22	2
8a	4.61, 4.65	5.82	9
9	5.82	4.61, 4.65	8a
10	5.89	5.72	11
11	5.72	2.65	12
		5.89	10
12	2.65	5.72	11
		1.16	12a
12a	1.16	2.65	12
14a	1.54	5.15	15
15	5.15	1.54	14a
		2.27	16
16	2.27	3.89	17
		5.15	15
17	3.89	0.85	18a
		2.27	16
18e	1.93	0.85	18a
		2.20	20e
		5.05	19
18a	0.85	1.93	18e
		3.89	17
		5.05	19
19	5.05	0.85	18a
		1.36	20a
		1.93	18e
		2.20	20e
20e	2.20	1.36	20a
		1.93	18e
		5.05	19
20a	1.36	2.20	20e
		5.05	19
22	5.75	2.29	24
		5.54	23
23	5.54	2.29	24
		5.75	22
24	2.29	1.63	26
		0.92	24a
		3.48	25
		5.54	23
		5.75	22
24a	0.92	2.29	24
25	3.48	2.29	24
26	1.63	0.94	26a
		2.29	24
26a	0.94	1.63	26
27	1.48–1.54	0.98	28
28	0.98	1.48–1.54	27
1′	4.75	1.70	2′a
2′e	2.08	1.70	2′a
		4.02	3′
2′a	1.70	2.08	2′e
		4.02	3′
		4.75	1′
3′	4.02	1.70	2′a
		2.08	2′e
		3.12	4′
4′	3.12	3.89	5′
		4.02	3′
5′	3.89	1.28	6′
		3.12	4′
6′	1.28	3.89	5′
1″	5.28	1.93	2″a
		2.21	2″e
2″e	2.21	1.93	2″a
		5.28	1″
2″a	1.93	2.21	2″e
		5.28	1″
3″	3.94	3.19	4″
4″	3.19	1.23	6″
		3.94	3″
		4.08	5″
5″	4.08	1.23	6″
		3.19	4″
6″	1.23	3.19	4″
		4.08	5″

synthetic gene cluster *avrBDCEFGHI* from *S. avermitilis*. The cluster, which contained a C-terminal portion of *ORF1*, was subcloned as an 8.7 kb *Nsi*I-*Hin*dIII fragment from pVE1190 behind the *ermE** promoter of pWHM1250.

A plasmid, pWHM481, was constructed in which the eight *avr* genes were divided into two groups: genes *avrB*, *avrE*, *avrD* and *avrC* in one, *avrI*, *avrH*, *avrG* and *avrF* in the other (Fig. 3C). The two sets of genes are each oriented in opposite directions and expressed under control of the *actI* and *actIII* promoters. The *avrB* and *avrE* genes were reoriented from the native arrangement into the same direction as *avrC* and *avrD* as follows: the polylinker LEH3 (see above) was synthesized and cloned into pNEB193 to create pWHM468 (Table 2), then *avrD* and *avrC* were cloned from pVE1190 as a 2.1 kb fragment into pWHM468 between the *Kpn*I and *Bst*EII sites to create pWHM469 (Table 2). The polylinker LEB4 containing a rbs and novel *Xba*I and *Avr*II restriction sites was introduced upstream of the start codon of *avrE* between the *Eco*RI and *Bam*HI sites of pWHM1251 [27] to create pWHM470. The *Avr*II-*Pst*I fragment containing the entire *avrE* gene was excised from pWHM470 and cloned into pWHM469 to create pWHM471 (Table 2). The *avrB* gene was amplified from pVE1190 by PCR with the primers PO6 and PO7 (above) as a 1.3 kb *Xba*I-*Avr*II fragment and cloned into pWHM468 to create pWHM472. The central portion of this fragment between *Sst*I and *Pml*I sites in pWHM472 was replaced with a non-amplified fragment from pVE1190 to produce pWHM473 (Table 2). The remaining ends of the *avrB* gene were sequenced to verify authenticity. The *Xba*I-*Avr*II fragment containing *avrB* was cloned from pWHM473 into pWHM471 to create pWHM474 (Table 2). The *Xba*I site was eliminated from pWHM474 to create pWHM479. The genes *avrB*, *avrC*, *avrD* and *avrE*, all oriented in the same direction, were cloned as a *Pac*I-*Eco*RI fragment from pWHM479 into pWHM467 under control

of the *act*I promoter to create pWHM480. The remaining genes *avrF*, *avrG*, *avrH*, and *avrI* were cloned from pVE1190 as two fragments (*Xho*I-*Nco*I and *Nco*I-*Not*I) into pANT841 to give pWHM476 (Table 2). This set was cloned from pWHM476 as a 4.2 kb *Bgl*II-*Spe*I fragment into pWHM468 to create pWHM477, before being introduced into pWHM480 as a 4.2 kb *Xba*I-*Nsi*I fragment under control of the *actIII* promoter to create pWHM481 (Table 2; Fig. 3C).

Modified versions of pWHM481 carrying an incomplete or partially disrupted set of *avr* sugar genes were generated. A plasmid with an in-frame deletion in the *avrH* gene was constructed as follows. A 2.1 kb *Xho*I-*Msc*I fragment, containing the genes *avrI* and *avrH* and part of *avrG* was subcloned from pWHM477, containing genes *avrIHGF*, into pSE380 to create pWHM2100. The same 2.1 kb *Hin*dIII-*Pst*I fragment from pWHM2100 was cloned into pWHM468 to create pWHM2101. An in-frame deletion removing a 693 bp fragment from *avrH* between *Bpu*11021 and *Stu*I sites was created in pWHM2101 to give pWHM2102. A 3.1 kb *Sst*I-*Msc*I fragment from pWHM477 was cloned into pSE380 to create pWHM2103. To replace the original *avrH* gene, a 1.4 kb *Msc*I-*Xho*I fragment from pWHM2102 with an in-frame deletion in *avrH* was cloned into pWHM2103 to create pWHM2104. To get plasmid 2105 with *avrIGFavr*Δ*H*, a 2.4 kb *Msc*I-*Sac*I fragment from pWHM2104 was cloned into pWHM477. Finally, to get a plasmid containing the *avrIGFavr*Δ*H* and *avrBEDC* cassettes, a 3.5 kb *Xba*I-*Nsi*I fragment from pWHM2105 was cloned into pWHM480 to create pWHM2106 (Table 2; Fig. 3C).

To construct a plasmid without the *avrB* gene, the *Xba*I site was eliminated from pWHM471, containing the *avrEDC* genes, to create pWHM2107, while a 3.25 kb *Pac*I-*Eco*RI fragment from pWHM2107 was cloned into pWHM467 to create pWHM2108. A 4.2 kb *Xba*I-*Nsi*I fragment from pWHM477, containing genes *avrIHGF*, was cloned into pWHM2108, containing *avrEDC*, to create pWHM2109 (Table 2; Fig. 3C).

A plasmid with an in-frame deletion in the *avrI* and *avrH* genes was constructed as follows. An in-frame deletion removed a 999 bp fragment from the *avrI* and *avrH* genes between the *Nco*I and *Msc*I sites in pWHM477 to give pWHM2110. A 3.2 kb *Xba*I-*Nsi*I fragment, containing the Δ*avrI* and Δ*avrH* genes and *avrG* and *avrF* was cloned into pWHM480, containing *avrBEDC*, to create pWHM2111 (Table 2; Fig. 3C).

A plasmid with deletion in *avrF* gene was constructed as follows. An in-frame deletion removing a 369 bp fragment from *avrF* gene between *Eco*47III and *Sst*I sites was created in pWHM477, containing the *avrIHGF* cassette, to give pWHM2129. From the latter plasmid, a 3.8 kb *Xba*I-*Nsi*I fragment, containing the *avrIHG* genes and Δ*avrF* gene, was cloned into pWHM480, containing the *avrBEDC* cassette, to create pWHM2130 (Table 2; Fig. 1B).

A plasmid with an in-frame deletion in the *avrI* gene was constructed using a 3.25 kb *Pml*I-*Nsi*I fragment, containing genes *avrHGF* and part of *avrI*, cloned from pWHM477 into Litmus28 to create pWHM2133, containing an in-frame deletion in the *avrI* gene. A 3.25 kb *Xba*I-*Nsi*I fragment from pWHM2133 was

Table 8
2D-NOESY couplings of avermectin A1a1 in methanol-d_4 (δ, relative to TMS)

Position	^{1}H	^{1}H	Position
2	3.22	5.47	3
3	5.47	1.79	4a
		3.22	2
4a	1.79	5.47	3
		3.95	5/6
5/6	3.95	1.79	4a
9	5.82	5.72	11
11	5.72	5.82	9
12	2.65	1.54	14a
		3.99	13
12a	1.16	3.99	13
13	3.99	1.16	12a
		1.54	14a
		2.65	12
14a	1.54	2.27	16
		2.65	12
		3.99	13
16	2.27	1.54	14a
18e	1.93	0.85	18a
18a	0.85	1.93	18e
20e	2.20	1.36	20a
20a	1.36	2.20	20e
22	5.75	0.92	24a
		2.29	24
		5.54	23
23	5.54	5.75	22
24	2.29	0.92	24a
		0.94	26a
		5.75	22
24a	0.92	2.29	24
		5.75	22
26	1.63	0.94	26a
26a	0.94	1.63	26
		2.29	24
2′e	2.08	4.02	3′
3′	4.02	2.08	2′e
4′	3.12	5.28	1″
		1.28	6′
5′	3.89	1.28	6′
6′	1.28	5.28	1″
		3.12	4′
		3.89	5′
1″	5.28	1.28	6′
		1.93	2″a
		3.12	4′
2″e	2.21	1.93	2″a
2″a	1.93	2.21	2″e
		3.19	4″
		3.94	3″
		5.28	1″
3″	3.94	1.93	2″a
		3.19	4″
4″	3.19	1.23	6″
		1.93	2″a
		3.94	3″
		4.08	5″
5″	4.08	1.23	6″
		3.19	4″
6″	1.23	3.19	4″
		4.08	5″

cloned into pWHM480, containing the *avrBEDC* genes, to create pWHM2134 (Table 2; Fig. 3C).

A plasmid with an in-frame deletion in the *avrI* gene and without the *avrE* gene was constructed as follows. A 3.25 kb *Xba*I-*Nsi*I fragment from pWHM2133, containing genes *avrHGF* and the Δ*avrI* gene, was cloned into pWHM2114, already containing genes *avrBDC*, to create pWHM2135 (Table 2; Fig. 3C).

To introduce additional genes (*eryBIII*, and *eryBV*) a two-plasmid system was used. pWHM467 contained the *avr* genes and thiostrepton resistance gene while pKOS025-129 carried the additional genes and hygromycin resistance marker. A derivative of pKOS025-129, containing the gene *eryBIII*, was constructed by cloning a 1.25 kb *Spe*I-*Not*I fragment, containing *eryBIII*, from pFL401 into pANT841 between the sites *Nhe*I and *Not*I to create pWHM488. A 1.25 kb *Hin*dIII-*Eco*RI fragment, containing *eryBIII* from pWHM488, was next cloned into pWHM485 to give pWHM2118. A 1.25 kb *Pac*I-*Nsi*I fragment from pWHM2118 was cloned into pKOS025-129 under control of the *actI* promoter, creating pWHM2119.

5.6. Bioconversion of avermectin aglycones and product analysis

Avermectin aglycones were produced by shaken-flask cultures of the *S. avermitilis* Δ1066 strain which has a 16 kb deletion of all the TDP-oleandrose biosynthesis genes except *avrB* [25], or *S. avermitilis* MA6057a, a mutant mapped to a deletion of the *avrF* gene, using previously described seed [47] and liquid production media [48].

Avermectin A1a aglycone was purified and characterized in the following way. The crude extract residues obtained by methanol and ethyl acetate extraction of recovered mycelia were fractionated over silica gel using a flash funnel method: 350 mg of crude extract residue coated on 5 g of silica gel in a 4 cm diameter, 4 cm

Table 9
HMBC couplings of avermectin A1a2 in methanol-d_4 (δ, relative to TMS)

Position	^{1}H	^{13}C	Position
4a	1.78	121.3	3
		134.8	4
5a	3.46	78.3	5/6
12a	1.20	41.0	12
		83.5	13
		138.4	11
14a	1.54	83.5	13
		119.6	15
		136.6	14
24a	0.92	31.8	24
		75.9	25
26a	0.94	28.6	27
		36.5	26
		75.9	25
28	0.98	28.6	27
		36.5	26
6′	1.23	64.3	5′
		76.6	4′
6″	1.24	69.8	5″
		78.8	4″

Table 10
H,H-COSY couplings of avermectin A1a2 in methanol-d_4 (δ, relative to TMS)

Position	^{1}H	^{1}H	Position
2	3.22	1.78	4a
3	5.47	1.78	4a
4a	1.78	3.22	2
		5.47	3
10	5.89	5.79	11
11	5.79	2.65	12
		5.89	10
12	2.65	1.20	12a
		5.79	11
12a	1.20	2.65	12
15	5.22	2.28	16
16	2.28	3.89	17
		5.22	15
17	3.89	0.84	18a
		2.28	16
18e	1.96	0.84	18a
18a	0.84	1.96	18e
		3.89	17
		5.05	19
19	5.05	0.84	18a
		1.35	20a
20e	2.17	1.35	20a
20a	1.35	2.17	20e
		5.05	19
22	5.74	5.54	23
23	5.54	5.74	22
24	2.29	0.92	24a
		3.48	25
24a	0.92	2.29	24
		3.48	25
25	3.48	0.92	24a
		2.29	24
26	1.63	0.94	26a
26a	0.94	1.63	26
27	1.47–1.54	0.98	28
28	0.98	1.47–1.54	27
1′	4.75	1.98	2′a
		2.15	2′e
2′e	2.15	1.98	2′a
		4.25	3′
		4.75	1′
2′a	1.98	2.15	2′e
		4.75	1′
3′	4.25	2.15	2′e
5′	4.29	1.23	6′
6′	1.23	4.29	5′
1″	5.10	1.62	2″a
2″e	2.18	1.62	2″a
2″a	1.62	2.18	2″e
		3.79	3″
		5.10	1″
3″	3.79	1.62	2″a
		2.95	4″
4″	2.95	3.65	5″
		3.79	3″
5″	3.65	1.24	6″
		2.95	4″
6″	1.24	3.65	5″

high scintered glass funnel was eluted with three successive methylene chloride washes, followed by elution with a 5% step gradient of ethyl acetate in methylene chloride and fractions of 20 ml were collected. The appropriate fractions from three such purifications were combined to give one sample of enriched avermectin A1a aglycone, which was further purified by semi-preparative HPLC using solvent gradient system 1 (see below). Alternatively avermectin A1a aglycone was isolated directly out of the crude extract residue in two purification steps by semi-preparative HPLC (solvent gradient system 2). The resulting purified material was analyzed by ESI-LRMS and ESI-HRMS as well as by HPLC comparison with authentic avermectin aglycone obtained through acid hydrolysis of a concentrated crude extract of avermectins obtained from fermentation of *S. avermitilis* ATCC 31272 (kindly provided by R.W. Fedechko and K. Stutzmann-Engwall at Chas. Pfizer and Co.).

For bioconversion experiments using *S. lividans* K4–114 harboring the pWHM481, pWHM2106, pWHM2109, pWHM2111, pWHM2130, pWHM2134, or pWHM2135 plasmids (Fig. 3C), or both pWHM2106 and pWHM2119 or both pWHM2109 and pWHM2122, transformants were grown on solid R2YE without sucrose with exogenous A1a avermectin aglycone (10 μg/ml). Antibiotics were added to the media as follows: for transformants carrying pWHM481, pWHM2106, pWHM2109, pWHM2111, pWHM2130, pWHM2134 and pWHM2135, thiostrepton at 30 μg/ml; for transformants carrying pWHM2106 and pWHM2119 or pWHM2109 and pWHM2122, thiostrepton at 30 μg/ml and hygromycin at 200 μg/ml. After 5 days of incubation, avermectin metabolites were extracted from chopped solid R2YE using equal volumes of ethyl acetate, concentrated by evaporation under a stream of nitrogen to give an oily residue, which was resuspended in methanol.

Our initial approach was to grow three agar plates of each strain. The methanol extracts of these were first analyzed by HPLC using the analytical system (see below) and those metabolites that showed the typical avermectin UV-absorption spectrum were isolated by semi-preparative HPLC (systems 1 and 3) before further being analyzed by electrospray mass spectrometry. The strains that were investigated in the above described manner are shown with positive ion ESI-MS *m/z* data for metabolites isolated from the respective strains and what possible product this (these) mass(es) might reflect in Table 3.

5.7. Isolation and characterization of avermectins A1a1, A1a2 and A1a3

Under the conditions described above *S. lividans* K4–114/pWHM2106, *S. lividans* K4–114/pWHM2111 and *S. lividans* K4–114/pWHM2130 strains were grown on 3 l, 1.5 l and 1.5 l of solid media (8.5 cm diameter plates, with each plate holding

Table 11
2D-NOESY couplings of avermectin A1a2 in methanol-d_4 (δ, relative to TMS)

Position	^{1}H	^{1}H	Position
3	5.47	1.78	4a
4a	1.78	5.47	3
5/6	3.93	3.46	5a
5a	3.46	3.93	5
10	5.89	5.79	11
11	5.79	5.89	10
12	2.65	1.54	14a
12a	1.20	4.05	13
13	4.05	1.20	12a
14a	1.54	2.65	12
18e	1.96	0.84	18a
18a	0.84	1.96	18e
20e	2.17	1.35	20a
20a	1.35	2.17	20e
22	5.74	0.92	24a
		5.54	23
23	5.54	5.74	22
24	2.29	0.92	24a
24a	0.92	2.29	24
		3.48	25
		5.74	22
25	3.48	0.92	24a
27	1.47–1.54	0.98	28
28	0.98	1.47–1.54	27
1′	4.75	1.98	2′a
		2.15	2′e
2′e	2.15	4.75	1′
		1.98	2′a
2′a	1.98	2.15	2′e
		4.75	1′
5′	4.29	1.23	6′
		5.10	1″
6′	1.23	4.29	5′
1″	5.10	4.29	5′
2″e	2.18	1.62	2″a
2″a	1.62	2.18	2″e
5″	3.65	1.24	6″
6″	1.24	3.65	5″

Table 12
HMBC couplings of avermectin A1a2 in chloroform-d_1 (δ, relative to TMS)

Position	^{1}H	^{13}C	Position
4a	1.81	118.3	3
		136.0	4
5/6	3.98	78.0	5/6
5a	3.50	77.9	5/6
12a	1.20	39.5	12
		82.0	13
		136.4	11
14a	1.51	82.0	13
		119.4	15
		134.5	14
18a	0.88	68.0	17
24a	0.91	30.6	24
		74.8	25
		136.3	22
26a	0.93	27.5	27
		35.3	26
28	0.95	27.5	27
		35.3	26
6′	1.27	62.7	3′
		75.1	4′
6″	1.30	68.0	5″
		78.4	4″

Table 13
H,H-COSY couplings of avermectin A1a2 in chloroform-d_1 (δ, relative to TMS)

Position	^{1}H	^{1}H	Position
2	3.31	1.81	4a
		3.98	5/6
		5.38	3
3	5.38	1.81	4a
		3.31	2
		3.98	5/6
4a	1.81	3.31	2
		5.38	3
5/6	3.98	3.31	2
		5.38	3
8a	4.62, 4.64	5.81	9
9	5.81	4.62, 4.64	8a
11	5.62	2.65	12
12	2.65	1.20	12a
		5.62	11
		4.05	13
12a	1.20	2.65	12
13	4.05	2.65	12
		2.29	16
		5.05	15
15	5.05	2.29	16
		4.05	13
16	2.29	3.86	17
		4.05	13
		5.05	15
17	3.86	2.29	16
		0.88	18a
18e	1.74	0.88	18a
18a	0.88	1.74	18e
		3.86	17
		5.36	19
19	5.36	1.48	20a
		2.03	20e
		0.88	18a
20e	2.03	1.48	20a
		5.36	19
20a	1.48	2.03	20e
		5.36	19
22	5.78	5.55	23
23	5.55	5.77	22
24	2.28	0.91	24a
		3.47	25
24a	0.91	2.28	24
25	3.47	2.28	24
26	1.60	0.93	26a
26a	0.93	1.48–1.54	27
		1.60	26
27	1.48–1.54	0.95	28
		0.93	26a
28	0.95	1.48–1.54	27
1′	4.83	1.92	2′a
2′e	2.14	1.92	2′a
		4.27	3′
2′a	1.92	2.14	2′e
		4.27	3′
		4.83	1′
3′	4.27	1.92	2′a
		2.14	2′e
4′	3.29	4.19	5′
5′	4.19	1.27	6′
		3.29	4′
6′	1.27	4.19	5′
1″	5.18	1.71	2″a
2″e	2.23	1.71	2″a
		3.95	3″
2″a	1.71	2.23	2″e
		3.95	3″
		5.18	1″
3″	3.95	1.71	2″a
		2.23	2″e
		3.19	4″
4″	3.19	3.67	5″
		3.95	3″
5″	3.67	1.30	6″
		3.19	4″
6″	1.30	3.67	5″

Table 14
2D-NOESY couplings of avermectin A1a2 in chloroform-d_1 (δ, relative to TMS)

Position	^{1}H	^{1}H	Position
3	5.38	1.81	4a
4a	1.81	5.38	3
12	2.65	1.20	12a
		1.51	14a
		4.05	13
12a	1.20	2.65	12
13	4.05	2.65	12
14a	1.51	2.65	12
15	5.05	2.29	16
16	2.29	5.05	15
19	5.36	2.03	20e
20e	2.03	1.48	20a
		5.36	19
20a	1.48	2.03	20e
1′	4.83	1.92	2′a
		2.14	2′e
2′e	2.14	1.92	2′a
		4.83	1′
2′a	1.92	2.14	2′e
		4.83	1′
3′	4.27	3.29	4′
4′	3.29	1.27	6′
		4.27	3′
5′	4.19	1.27	6′
6′	1.27	4.19	5′
		3.29	4′
1″	5.18	1.71	2″a
		2.23	2″e
2″e	2.23	5.18	1″
		3.95	3″
2″a	1.71	5.18	1″
3″	3.95	2.23	2″e
5″	3.67	1.30	6″
6″	1.30	3.67	5″

about 25 ml material), respectively. The plates were chopped and extracted four times with ethyl acetate and three times with methanol, before evaporating the combined extracts of each strain to dryness. The avermectins A1a2 and A1a3 were separated out of the crude extracts from avermectin A1a1 by semi-preparative HPLC (system 4, see below). By using the same semi-preparative HPLC treatment a second time, purified avermectin A1a1 was obtained. Avermectin A1a2 was separated from a third compound by preparative thin-layer chromatography (silica gel 60/F254 TLC plates, E. Merck, Darmstadt, Germany; ethyl acetate:methylene chloride:acetonitrile 50:100:8) and extracted from the scraped off silica gel by ethyl acetate and methanol, before purifying the compounds on Sephadex LH20 (Pharmacia; solvent methanol). The third compound also showed the typical avermectin UV-spectrum and the mass determined to be the same as that of avermectins A1a1 and A1a2. Avermectin A1a3 was purified out of its crude extract by two semi-preparative HPLC steps using system 2. We received 0.5 mg/l of avermectin A1a1, 0.4 mg/l avermectin A1a2, and 0.3 mg/l for the third avermectin derivative from both *S. lividans* K4–114/pWHM2106 (*avrBEDCIGF*, Δ*avrH*) and *S. lividans* K4–114/pWHM2111 (*avrBEDCGF*, Δ*avrHI*) as well as 1.1 mg/l avermectin A1a3 from *S. lividans* K4–114/pWHM2130 (*avrBEDCIHG*, Δ*avrF*).

5.8. Avermectin A1a1

$M = 859.06$ ($C_{47}H_{70}O_{14}$); ESI-MS pos. mode *m/z*: 881.5 [(M+Na)$^+$]; MP: 171°C; IR (KBr): ∇ = 3487, 2994, 2935, 2866, 1381, 1368, 1365, 1157, 1148, 1125, 1065, 1055, 1030, 991, 975, 956, 803, 615, 470, 419, 393 cm^{-1}; UV (methanol) max nm: 236.0, 243.5, 252.7; R_f: 0.17 (ethyl acetate:methylene chloride:acetonitrile 50:100:8; R_f avermectin A1a aglycone 0.67); R_f 17.49 min (analytical HPLC system; R_f avermectin A1a aglycone 12.95 min); NMR data see Tables 4–8.

Table 15
HMBC couplings of avermectin A1a3 in methanol-d_4 (δ, relative to TMS)

Position	^{1}H	^{13}C	Position
4a	1.78	121.2	3
		135.2	4
5a	3.46	78.2	5/6
12a	1.12	84.0	13
		139.0	11
14a	1.53	84.0	13
		119.2	15
		137.2	14
18a	0.86	69.9	19
		70.1	17
20a	1.35	69.9	19
		97.3	21
22	5.75	97.3	21
24a	0.92	31.8	24
		75.9	25
		136.6	22
26a	0.94	28.5	27
		36.6	26
		75.9	25
28	0.99	28.5	27
		36.6	26
4′	2.91	72.5	3′
6′	1.26	73.2	5′
		78.7	4′

Table 16
H,H-COSY couplings of avermectin A1a3 in methanol-d_4 (δ, relative to TMS)

Position	^{1}H	^{1}H	Position
2	3.21	1.78	4a
3	5.47	1.78	4a
4a	1.78	3.21	2
		5.47	3
8a	4.60–4.64	5.80	9
9	5.80	4.60–4.64	8a
10	5.86	5.65	11
11	5.65	2.60	12
		5.86	10
12	2.60	1.12	12a
		5.65	11
		4.09	13
12a	1.12	2.60	12
13	4.09	2.60	12
14a	1.53	5.24	15
15	5.24	1.53	14a
		2.26	16
16	2.26	5.24	15
		3.89	17
17	3.89	2.26	16
18e	1.92	0.86	18a
18a	0.86	1.92	18e
19	5.04	1.35	20a
		2.19	20e
20e	2.19	1.60	20a
		5.04	19
20a	1.35	2.19	20e
		5.04	19
22	5.75	5.54	23
23	5.54	5.75	22
24	2.29	0.92	24a
		3.46	25
24a	0.92	2.29	24
25	3.46	2.29	24
26	1.65	0.94	26a
26a	0.94	1.65	26
27	1.48–1.58	0.99	28
28	0.99	1.48–1.58	27
1′	4.38	1.60	2′a
2′e	2.14	1.60	2′a
		3.48	3′
2′a	1.60	2.14	2′e
		4.38	1′
3′	3.48	2.14	2′e
		2.91	4′
4′	2.91	3.48	3′
		3.14	5′
5′	3.14	1.26	6′
		2.91	4′
6′	1.26	3.14	5′

5.9. Avermectin A1a2

$M = 859.06$ ($C_{47}H_{70}O_{14}$); ESI-MS pos. mode *m/z*: 881.5

[(M+Na)$^+$]; mp: 169°C; IR (KBr): ν = 3480, 2985, 2930, 2860, 1376, 1364, 1360, 1150, 1141, 1119, 1060, 1046, 1022, 985, 967, 950, 794, 607, 467, 415, 393 cm^{-1}; UV (methanol) max nm: 236.0, 243.5, 252.7; R_f: 0.15 (ethyl acetate:methylene chloride: acetonitrile 50:100:8; R_f avermectin A1a aglycone 0.67); R_f 18.49 min (analytical HPLC system; R_f avermectin A1a aglycone 12.95 min); NMR data see Tables 4, 5, 9–14.

5.10. Avermectin A1a3

M = 728.92 ($C_{41}H_{60}O_{11}$); ESI-MS pos. mode m/z: 751.6 [(M+Na)$^+$]; mp: 140°C; IR (KBr): ν = 3420, 2981, 2921, 2839, 1722, 1625, 1370, 1355, 1328, 1154, 1146, 1115, 1062, 990, 902, 795, 586, 468, 417, 391 cm^{-1}; UV (methanol) max nm: 236.0, 243.5, 252.7; R_f: 0.27 (ethyl acetate:methylene chloride:acetonitrile 50:100:8; R_f avermectin A1a aglycone 0.67); R_f 14.24 min (analytical HPLC system; R_f avermectin A1a aglycone 12.95 min); NMR data see Tables 4, 5, 15 and 16.

5.11. HPLC

A Waters HPLC system (controlled by Millenium^{32} software, v. 3.5) with two pumps (models 510 and 515), pump control module, and photodiode array detector (model 996) was used. For analytical purposes we used a Nova-Pak C18 60A 4 μm (150×3.9 mm) column with 1.0 ml/min flow speed and the following solvent system: solvent A = water; solvent B = methanol; flow rate of 1.0 ml/min, ambient temperature, 30% A:70% B to 10% A:90% B (linear gradient, curve 6, 0–20 min); 10% A:90% B to 100% B (concave gradient, curve 9, 20–25 min); 100% B to 30% A:70% B (curve 9, 25–30 min). For semi-preparative fractioning several different solvent gradients were developed, using water as solvent A, methanol as solvent B and a flow rate of 2 ml/min: System 1: 30% A:70% B to 100% B (curve 6, 0–40 min); 100% B to 30% A:70% B (curve 9, 40–50 min). System 2: 30% A:70% B to 40% A:60% B (curve 6, 0–60 min); 40% A:60% B to 30% A:70% B (curve 6, 60–62 min). System 3: 30% A:70% B to 10% A:90% B (curve 6, 0–40 min); 10% A:90% B to 100% B (curve 6, 40–45 min); 100% B to 30% A:70% B (curve 6, 45–50 min). System 4: 30% A:70% B to 12.5% A:87.5% B (curve 6, 0–110 min); 12.5% A:87.5% B to 100% B (curve 6, 110–115 min); 100% B to 30% A:70% B (curve 6, 115–120 min). For both analytical and semi-preparative work Sentry Guard Columns Nova-Pak C18 60A 4 μm (20×3.9 mm) were used in addition.

5.12. Additional instruments

The ^{1}H and ^{13}C NMR spectra were recorded in methanol and chloroform at 500 and 125.71 MHz, respectively. The different structures were elucidated by using 1D spectra and 2D homo- and heteronuclear correlation experiments (^{1}H, ^{13}C, DEPT, H,H-COSY, HMQC, HSQC, HMBC, 2D-NOESY, 1D-NOESY, 1D-TOCSY) recorded on a Varian Unity-500. Electrospray ionization mass spectrometry (ESI-MS, University of Wisconsin Biotechnology Center) and matrix-assisted laser desorption/ionization mass spectrometry (HR-MALDI-FT-MS, Mass Consortium, San Diego, CA, USA) was used to determine the mass. IR-spectra were recorded on a Perkin-Elmer Infrared Spectrometer 599 B. A Unimelt Thomas Hoover Capillary Melting Point Apparatus was used to determine melting points and PCR amplification was performed in a thermal cycler Perkin-Elmer Cetus model 480.

Acknowledgements

We thank Jon T. Roll for construction of the modified pRM5 vector, pWHM467, and Charles G. Fry for excellent help using the NMR instrumentation. This work was supported in part by a Grant from the National Institutes of Health (GM31925). The NMR spectra obtained in the Chemistry and Biochemistry Departments at the University were determined on instruments supported by Grants from the NSF (CHE-8813550 and CHE-9629688) and NIH (S10 RR04981-01).

References

[1] D.J. MacNeil, Avermectins, in: L.C. Vining, C. Stuttard (Eds.), Genetics and Biochemistry of Antibiotic Production, Butterworth-Heinemann, Boston, MA, 1995, pp. 421–442.
[2] H. Ikeda, S. Omura, Avermectin biosynthesis, Chem. Rev. 97 (1997) 2591–2609.
[3] H.G. Davies, R.H. Green, Avermectins and milbemycins, Nat. Prod. Rep. 3 (1986) 87–121.
[4] Q.A. McKellar, H.A. Benchaoui, Avermectins and milbemycins, J. Vet. Pharmacol. Ther. 19 (1996) 331–351.
[5] A. Kirschning, A.F.-W. Bechthold, J. Rohr, Chemical and biochemical aspects of deoxysugars and deoxysugar oligosaccharides, Top. Curr. Chem. 188 (1997) 1–84.
[6] D.A. Johnson, H.-w. Liu, Mechanisms and pathways from recent deoxysugar biosynthesis research, Curr. Opin. Chem. Biol. 2 (1998) 642–649.
[7] T.M. Hallis, H.-w. Liu, Learning nature's strategies for making deoxy sugars: pathways, mechanisms, and combinatorial applications, Acc. Chem. Res. 32 (1999) 579–598.
[8] A. Trefzer, J.A. Salas, A. Bechthold, Genes and enzymes involved in deoxysugar biosynthesis in bacteria, Nat. Prod. Rep. 16 (1999) 283–299.
[9] D.J. MacNeil, K.M. Gewain, C.L. Ruby, G. Dezeny, P.H. Gibbons, T. MacNeil, Analysis of *Streptomyces avermitilis* genes required for avermectin biosynthesis utilizing a novel integration vector, Gene 111 (1992) 61–68.
[10] M.D. Schulman, D. Valentino, O. Hensens, D. Zink, M. Nallin, L. Kaplan, D.A. Ostlind, Demethylavermectins. Biosynthesis, isolation and characterization, J. Antibiot. 38 (1985) 1494–1498.
[11] H. Ikeda, H. Kotaki, S. Omura, Genetic studies of avermectin biosynthesis in *Streptomyces avermitilis*, J. Bacteriol. 169 (1987) 5615–5621.
[12] J.L. Occi, K.M. Gerwain, C.L. Ruby, D.J. MacNeil, Cloning and sequencing a nine kb region from *Streptomyces avermitilis* essential for glycosylation of avermectin, Abstracts of the annual meeting of the society for industrial microbiology, P49, 1991, p. 93, Philadelphia, PA.
[13] H. Ikeda, T. Nonomiya, M. Usami, T. Ohta, S. Omura, Organization of the biosynthetic gene cluster for the polyketide anthelmintic macrolide avermectin in *Streptomyces avermitilis*, Proc. Natl. Acad. Sci. USA 96 (1999) 9509–9514.
[14] H. Ikeda, S. Omura, Control of avermectin biosynthesis in *Strepto-*

myces avermitilis for the selective production of a useful component, J. Antibiot. 48 (1995) 549–562.

[15] R.G. Summers, S. Donadio, M. Staver, E. Wendt-Pienkowski, C.R. Hutchinson, L. Katz, Sequencing and mutagenesis of genes from the erythromycin biosynthetic gene cluster of *Saccharopolyspora erythraea* that are involved in L-mycarose and D-desosamine production, Microbiology 143 (1997) 3251–3262.

[16] S. Gaisser, G.A. Böhm, J. Cortés, P.F. Leadlay, Analysis of seven genes from the *eryAI-eryK* region of the erythromycin biosynthetic gene cluster in *Saccharopolyspora erythraea*, Mol. Gen. Genet. 256 (1997) 239–251.

[17] S. Gaisser, G.A. Böhm, M. Boumith, M.C. Raynal, N. Dhillon, J. Cortes, P.F. Leadlay, Analysis of *eryBI*, *eryBIII* and *eryBVII* from the erythromycin biosynthetic gene cluster in *Saccharopolyspora erythraea*, Mol. Gen. Genet. 258 (1998) 78–88.

[18] K. Salah-Bey, M. Dourmith, J.-M. Michel, S. Haydock, J. Cortes, P.F. Leadlay, M.C. Raynal, Targeted gene inactivation for the elucidation of deoxysugar biosynthesis in the erythromycin producer *Saccharopolyspora erythraea*, Mol. Gen. Genet. 257 (1998) 542–553.

[19] H. Chen, Z. Guo, H.-w. Liu, Expression, purification, and characterization of TylM1, an *N*,*N*-dimethyltransferase involved in the biosynthesis of mycaminose, J. Am. Chem. Soc. 120 (1998) 9951–9952.

[20] H. Chen, G. Agnihotri, Z. Guo, N.L.S. Que, X.H. Chen, H.-w. Liu, Biosynthesis of mycarose: Isolation and characterization of enzymes involved in the C-2 deoxygenation, J. Am. Chem. Soc. 121 (1999) 8124–8125.

[21] C. Olano, A.M. Rodriguez, J.-M. Michel, C. Mendez, M.-C. Raynal, J.A. Salas, Analysis of a *Streptomyces antibioticus* chromosomal region involved in oleandomycin biosynthesis, which encodes two glycosyltransferases responsible for glycosylation of the macrolactone ring, Mol. Gen. Genet. 259 (1998) 299–308.

[22] G. Draeger, S.H. Park, H.G. Floss, Mechanism of the 2-deoxygenation step in the biosynthesis of the deoxyhexose moieties of the antibiotics granaticin and oleandomycin, J. Am. Chem. Soc. 121 (1999) 2611–2612.

[23] I. Aguirrez-Balaga, C. Olano, N. Allende, L. Rodriguez, A. Brana, C. Mendez, J. Salas, Identification and expression of genes involved in biosynthesis of L-oleandrose and its intermediate L-olivose in the oleandomycin producer *Streptomyces antibioticus*, Antimicrob. Agents Chemother. 44 (2000) 1266–1275.

[24] M.D. Schulman, S.L. Acton, D.L. Valentino, B.H. Arison, Purification and identification of dTDP-oleandrose, the precursor of the oleandrose units of the avermectins, J. Biol. Chem. 265 (1990) 16965–16970.

[25] T. MacNeil, K.M. Gewain, D. MacNeil, Deletion analysis of the avermectin biosynthetic genes of *Streptomyces avermitilis* by gene cluster displacement, J. Bacteriol. 175 (1993) 2552–2563.

[26] M.D. Schulman, D. Valentino, S. Streicher, C. Ruby, *Streptomyces avermitilis* mutants defective in methylation of avermectins, Antimicrob. Agents Chemother. 31 (1987) 744–747.

[27] K. Madduri, J. Kennedy, G. Rivola, A. Inventi-Solari, S. Filippini, G. Zanuso, A.L. Colombo, K.M. Gewain, J.L. Occi, D.J. MacNeil, C.R. Hutchinson, Production of the antitumor drug epirubicin (4′-epidoxorubicin) and its precursor by a genetically engineered strain of *Streptomyces peucetius*, Nat. Biotechnol. 16 (1998) 69–74.

[28] M.J. Bibb, J. White, J.M. Ward, G.R. Janssen, The mRNA for the 23S rRNA methylase encoded by the *ermE* gene of *Saccharopolyspora erythraea* is translated in the absence of a conventional ribosome-binding site, Mol. Microbiol. 14 (1994) 533–545.

[29] J. Vara, M. Lewandowska-Skarbek, Y.G. Wang, S. Donadio, C.R. Hutchinson, Cloning of genes governing the deoxysugar portion of the erythromycin biosynthetic pathway in *Saccharopolyspora erythraea* (*Streptomyces erythreus*), J. Bacteriol. 171 (1989) 5872–5881.

[30] R. McDaniel, S. Ebert-Khosla, D.A. Hopwood, C. Khosla, Engineered biosynthesis of novel polyketides, Science 262 (1993) 1546–1550.

[31] R. Ziermann, M.C. Betlach, Recombinant polyketide synthesis in *Streptomyces*: engineering of improved host strains, BioTechniques 26 (1999) 106–110.

[32] H. Decker, S. Haag, G. Udvarnoki, J. Rohr, Novel genetically engineered tetracenomycins, Angew. Chem. Int. Ed. Engl. 34 (1995) 1107–1110.

[33] L. Zhao, D.H. Sherman, H.-w. Liu, Biosynthesis of desosamine: construction of a new methymycin/neomethymcyin analogue by deletion of a desosamine biosynthetic gene, J. Am. Chem. Soc. 120 (1998) 10256–10257.

[34] S.-E. Wohlert, G. Blanco, F. Lombo, E. Fernandez, A.F. Brana, S. Reich, G. Udvarnoki, C. Mendez, H. Decker, J. Frevert, J.A. Salas, J. Rohr, Novel hybrid tetracenomycins through combinatorial biosynthesis using a glycosyltransferase encoded by the *elm* genes in cosmid 16F4 and which shows a broad sugar substrate specificity, J. Am. Chem. Soc. 120 (1998) 10596–10601.

[35] S.A. Borisova, L. Zhao, D.H. Sherman, H.-w. Liu, Biosynthesis of desosamine: construction of a new macrolide carrying a genetically designed sugar moiety, Org. Lett. 1 (1999) 133–136.

[36] L. Zhao, J. Ahlert, Y. Xue, J.S. Thorson, D.H. Sherman, H.-w. Liu, Engineering a methymycin/pikromycin-calicheamycin hybrid: construction of two new macrolides carrying a designed sugar moiety, J. Am. Chem. Soc. 121 (1999) 9881–9882.

[37] E. Künzel, B. Faust, C. Oelkers, U. Weissbach, D.W. Bearden, G. Weitnauer, L. Westrich, A. Bechthold, J. Rohr, Inactivation of the urdGT2 gene, Which encodes a glycosyltransferase responsible for the C-glycosyltransfer of activated D-olivose, leads to formation of the novel urdamycins I, J, and K, J. Am. Chem. Soc. 121 (1999) 11058–11062.

[38] H. Yamase, L. Zhao, H.-w. Liu, Engineering a hybrid sugar biosynthesis pathway: Production of L-rhamnose and its implication on dihydrostreptose biosynthesis, J. Am. Chem. Soc. 122 (2000) 12397–12398.

[39] C. Olano, N. Lomovskaya, L. Fonstein, J.T. Roll, C.R. Hutchinson, A two-plasmid system for the glycosylation of polyketide antibiotics: bioconversion of ε-rhodomycinone to rhodomycin D, Chem. Biol. 6 (1999) 845–855.

[40] R. McDaniel, A. Thamchaipenet, C. Gustafsson, H. Fu, M. Betlach, M. Betlach, G. Ashley, Multiple genetic modifications of the erythromycin polyketide synthase to produce a library of novel 'unnatural' natural products, Proc. Natl. Acad. Sci. USA 96 (1999) 1846–1851.

[41] Q. Xue, G. Ashley, C.R. Hutchinson, D.V. Santi, A multi-plasmid approach to preparing large libraries of polyketides, Proc. Natl. Acad. Sci. USA 96 (1999) 11740–11745.

[42] P.J. Solenberg, P. Matsushima, D.R. Stack, S.C. Wilkie, R.C. Thompson, R.H. Baltz, Production of hybrid glycopeptide antibiotics *in vitro* and in *Streptomyces toyocaensis*, Chem. Biol. 4 (1997) 195–202.

[43] P.A. Patten, R.J. Howard, W.P.C. Stemmer, Applications of DNA shuffling to pharmaceuticals and vaccines, Curr. Opin. Biotechnol. 8 (1997) 724–733.

[44] J. Sambrook, E.F. Fritsch, T. Maniatis, Molecular Cloning: A Laboratory Manual, 2nd edn., Cold Spring Harbor Laboratory Press, Cold Spring Harbor, NY, 1989.

[45] K.M. Gerwain, J.L. Occi, F. Foor, D.J. MacNeil, Vectors for generating nested deletions and facilitating subclongin G+C-rich DNA between *Escherichia coli* and *Streptomyces* sp., Gene 119 (1992) 149–150.

[46] D.A. Hopwood, M.J. Bibb, C.P. Smith, J.M. Ward, H. Schrempf, Genetic Manipulation of *Streptomyces*: A Laboratory Manual, The John Innes Foundation, Norwich, 1985.

[47] R.W. Burg, B.M. Miller, E.E. Baker, J. Birnbaum, S.A. Currie, R. Hartman, Y.L. Kong, R.L. Monaghan, G. Olson, I. Putter, J.B. Tunac, H. Wallick, E.O. Stapley, R. Oiwa, S. Omura, Avermectins, new family of potent anthelmintic agents: producing organism and fermentation, Antimicrob. Agents Chemother. 15 (1979) 361–367.

[48] T.S. Chen, B.H. Arison, V.P. Gullo, E.S. Inamine, Further studies on the biosynthesis of avermectins, J. Ind. Microbiol. 4 (1989) 231–237.